AGU PUBLICATIONS

JGR

Journal of Geophysical Research: Solid Earth

RESEARCH ARTICLE
10.1002/2013JB010890

Key Points:
- Velocity structure of the Apennines is determined by a multiscale tomography
- Large Cenozoic mafic intrusions are identified in the Apulian crust
- Pressurized CO_2 reservoirs identified under the belt can affect seismicity

Supporting Information:
- Readme
- Figure S1
- Figure S2
- Figure S3
- Table S1
- Table S2

Correspondence to:
L. Improta,
luigi.improta@ingv.it

Citation:
Improta, L., P. De Gori, and C. Chiarabba (2014), New insights into crustal structure, Cenozoic magmatism, CO_2 degassing, and seismogenesis in the southern Apennines and Irpinia region from local earthquake tomography, *J. Geophys. Res. Solid Earth*, *119*, 8283–8311, doi:10.1002/2013JB010890.

Received 3 DEC 2013
Accepted 4 OCT 2014
Accepted article online 12 OCT 2014
Published online 14 NOV 2014

New insights into crustal structure, Cenozoic magmatism, CO_2 degassing, and seismogenesis in the southern Apennines and Irpinia region from local earthquake tomography

Luigi Improta[1], Pasquale De Gori[1], and Claudio Chiarabba[1]

[1]Istituto Nazionale di Geofisica e Vulcanologia, Rome, Italy

Abstract We present high-resolution *Vp* and *Vp/Vs* models of the southern Apennines (Italy) computed using local earthquakes recorded from 2006 to 2011 with a graded inversion scheme that progressively resolves the crustal structure, from the large scale of the Apennines belt to the local scale of the normal fault system. High-*Vp* bodies defined in the upper crust and midcrust under the external Apennines are interpreted as extensive mafic intrusions revealing anorogenic magmatism episodes that broadened on the Adriatic domain during Paleogene. Under the mountain belt, a low-*Vp* region, annular to the Neapolitan volcanic district, indicates the existence of a thermal/fluid anomaly in the midcrust, coinciding with a shallow Moho and diffuse degassing of deeply derived CO_2. In the belt axial zone, low-*Vp/Vs* gas-pressurized rock volumes under the Apulian carbonates correlate to high heat flow, strong CO_2-dominated gas emissions of mantle origin, and shallow carbonate reservoirs with pressurized CO_2 gas caps. We hypothesize that the pressurized fluid volumes located at the base of the active fault system influence the rupture process of large normal faulting earthquakes, like the 1980 *Mw*6.9 Irpinia event, and that major asperities are confined within the high-*Vp* Apulian carbonates. This study confirms once more that preexisting structures of the Pliocene Apulian belt controlled the rupture propagation during the Irpinia earthquake. The main shock broke a ~30 km long, NE dipping seismogenic structure, whereas delayed ruptures (both the 20 s and the 40 s subevents) developed on antithetic faults, reactivating thrust faults located at the eastern edge of the Apulian belt.

1. Introduction

The southern Apennines is a Miocene-early Pleistocene NE directed thrust belt originated by the deformation of the Adria continental margin during the eastward retreat of the subducting Ionian/Adria slab (Figure 1) [*Malinverno and Ryan*, 1986; *Dewey et al*., 1989; *Patacca et al*., 1990; *Doglioni et al*., 1996; *Faccenna et al*., 2001]. The range consists of a stack of rootless nappes, incorporating sedimentary units of the Adria passive margin, that overthrusts carbonate thrust sheets of the Apulia Platform (AP) (Figure 1). During the process of retreat, thrust propagation in the external belt coexisted with extension in the Tyrrhenian back-arc basin and crustal thinning along the Tyrrhenian margin (*Patacca et al*. [1990], among others). Since middle Pleistocene, SW-NE regional extension in the axial belt [*Cinque et al*., 1993] has been accompanied by volcanism along the Tyrrhenian margin, whose potassic and ultrapotassic magmas indicate a metasomatized mantle source [*Avanzinelli et al*., 2009, and references therein]. Anomalous and strongly hydrated mantle is also the source of massive and diffuse nonvolcanic CO_2 degassing at the surface that characterizes the western part of the southern Apennines (e.g., Campanian Degassing Structure) [*Chiodini et al*., 2004].

In spite of extensive geophysical studies motivated by the high hydrocarbon potential, the deep structure and tectonic evolution of the thrust belt (e.g., thin- versus thick-skinned tectonics) are still debated [*Improta and Corciulo*, 2006, and references therein]. Consequently, the degree of involvement of the crystalline basement in the thrust belt is still unconstrained, and the relation between deep and shallow structures of the crust is unclear.

Quaternary extension has generated a large normal fault system that dissects the mountain range. Historical earthquakes [*CPTI Working Group*, 2004] and instrumental seismicity [*Chiarabba et al*., 2005] define an almost

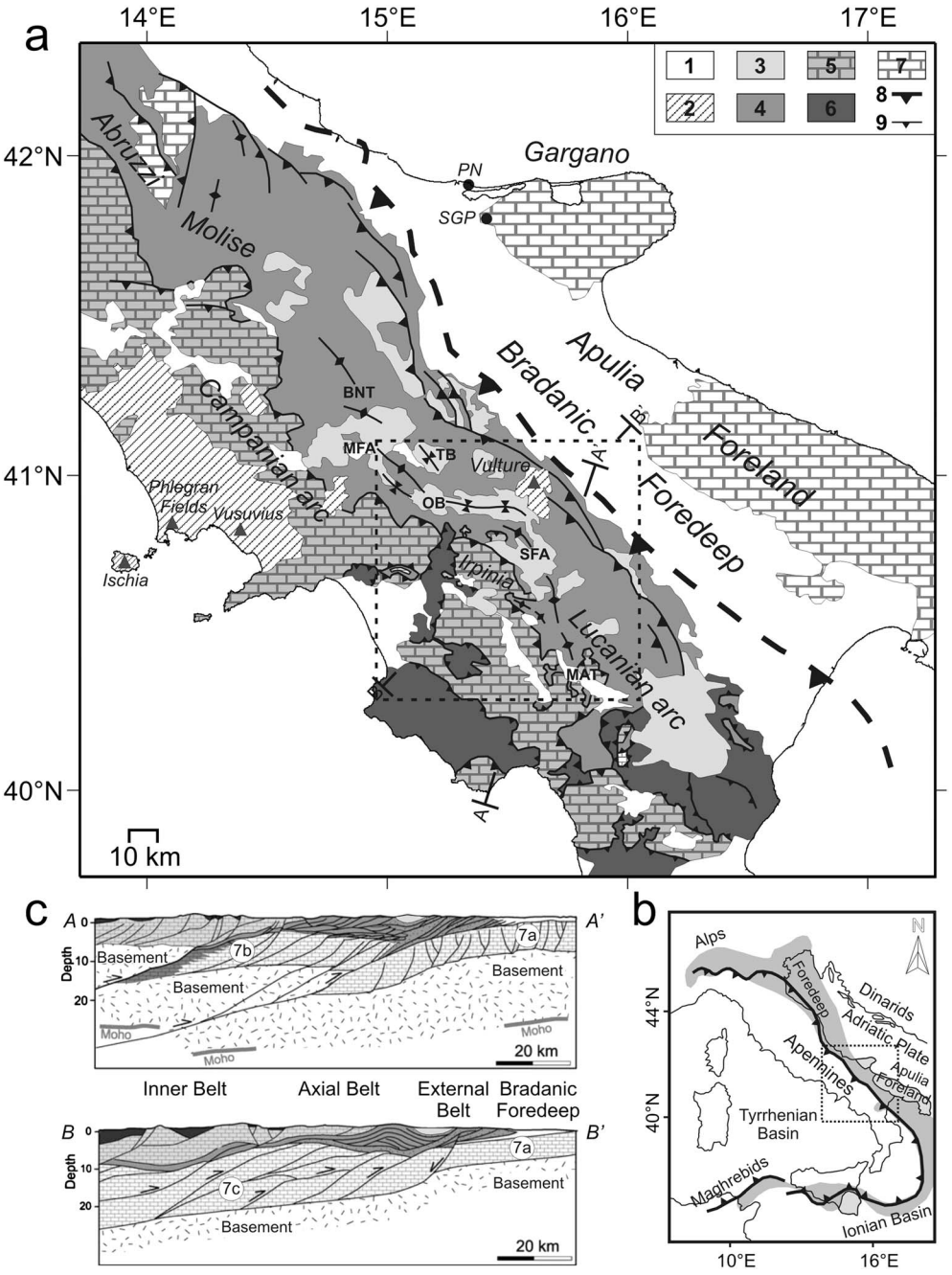

Figure 1. (a) Simplified geologic map of southern Apennines and surrounding regions. 1, Quaternary deposits; 2, middle Pleistocene to present volcanics; 3, Pliocene to early Pleistocene thrust-sheet-top satellite basins; 4, Meso-Cenozoic Lagonegro basin sequences; 5, Meso-Cenozoic carbonates of the Apeninnic platform, including Miocene flysch deposits; 6, Paleogene to lower Miocene basin sequences of internal nappes; 7, Mesozoic-Tertiary carbonates of the Apulia Platform (AP); 8, buried frontal ramp of the Apennines; and 9, main reverse faults. Triangles denote Quaternary volcanoes, black dots the small Paleogene mafic intrusions of the AP (PN = Pietre Nere and SGP = S. Giovanni in Pane). Labels are BNT = Benevento Trend, MFA = Mount Forcuso antiform, OB = Ofanto Basin, TB = Trevico Basin, SFA = S. Fele antiform, and MAT = Mount Alpi Trend. The dashed line bounds the Irpinia model. Regional map of the main domains in central Mediterranean that outlined the area investigated in this study. (c) Conflicting models of the deep structure of the southern Apennines based on thick-skinned (section A-A', modified after *Menardi Noguera and Rea* [2000]) and thin-skinned tectonic interpretations (section B-B', corresponding to the CROP-04 profile, is modified from *Mazzotti et al.* [2000]). Labels: 7a = Outer AP, 7b = Inner AP involved in the buried Apulian belt, and 7c = Apulia carbonate duplex system.

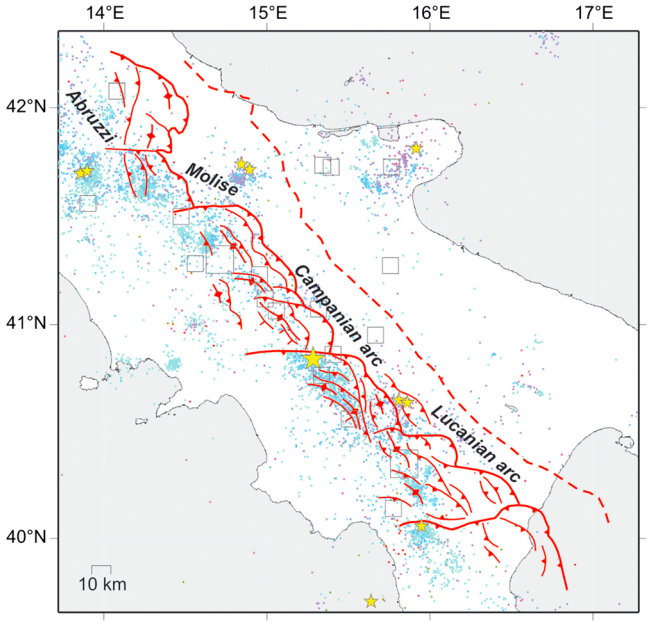

Figure 2. Seismicity map of southern Italy. Small dots are the instrumental earthquakes recorded by the Rete Sismica Nazionale Centralizzata (RSNC) during the past 30 years, with largest events (M_L >5) depicted by stars [*Chiarabba et al.*, 2005]. The largest star is the epicenter of the 1980 *Mw*6.9 Irpinia event. Squares indicate historical events with magnitude greater than 6.0 [*CPTI Working Group*, 2004]. The map also reports the main structural lineaments (thrusts, anticlines, and normal faults) at the top of the AP, with the buried frontal ramp of the AP belt outlined by a thicker yellow line (redrawn from *Nicolai and Gambini* [2007]). The dashed line corresponds to the buried front of the Apennines belt.

continuous NW trending, and 15 km thick seismic belt (Figure 2) along which 3–5 mm/yr of extension observed across the mountain range is accommodated [*D'Agostino et al.*, 2008]. During the past 300 years, several devastating earthquakes struck the range, causing more than 42,000 victims and making the southern Apennines one of the regions with the higher seismic hazard of central Mediterranean [*Marzocchi et al.*, 2012]. The *M*7 maximum magnitude of recent and historical earthquakes demands the segmentation of the normal fault system in distinct smaller faults that have a scale of a few tens of kilometers. One of the main issues still unsolved is which factors control this fault segmentation.

In this study, we use high-quality *P* and S waves arrival times of local and regional events, recorded by the recently improved broadband seismic network of the Istituto Nazionale di Geofisica e Vulcanologia (INGV), to compute the first high-resolution tomographic picture of southern Apennines that samples almost the entire middle and upper crusts. The primary goal is to find new constraints on the crustal structure of the belt, complementing field geology and subsurface exploration data, for addressing the tectonic evolution of the Apennines. To do this, regional-scale data yield a desired illumination underneath the AP, whose top is generally well defined in industry reflection profiles but its base is only seen locally [*Shiner et al.*, 2004].

Additionally, the definition of a high-resolution velocity model of the extensional seismic belt is a prerequisite for investigating the seismogenic normal faulting system and the factors that control its lateral segmentation. *Vp* and *Vp*/*Vs* models permit to define lateral crustal heterogeneities and the presence of fluids within the crust, whose role seems to be crucial in the seismogenesis of Apennines [*Miller et al.*, 2004]. We focus on the Irpinia region, struck in 1980 by the strongest event (*Mw* 6.9) of the past century in southern Apennines. This region is selected for two main reasons: (i) the quite good knowledge of the source mechanism of the 1980 earthquake [*Giardini et al.*, 1996, and references therein] and (ii) the availability of high-quality local data recorded by numerous seismic stations operating in the area since 2005, belonging to the INGV network and to the Irpinia Seismic Network (ISNet) local network [*Iannaccone et al.*, 2010]. By combining regional and local dense data in a graded tomographic scheme, we obtain an upgraded picture of the velocity structure at a 2 to 3 km of vertical and horizontal scale, in a broad region surrounding the source of the 1980 earthquake.

With respect to previous [*Amato et al.*, 1992] and recently published local earthquake tomography of the Irpinia fault area [*Amoroso et al.*, 2014], our study permits to resolve a broader crustal volume, thanks to the use of both regional and local data and to the graded approach of our tomographic procedure. The result is a high spatial resolution model of the Irpinia region embedded in a high definition regional model of southern Apennines, resolved for the upper and middle crusts. In addition, interpretation of our models is based on subsurface constraints from hydrocarbon exploration and on the comparison with published magnetic, magnetotelluric, heat flow and geochemical data.

2. Geologic Setting of the Southern Apennines

Structural regional synthesis of the southern Apennines featured since the 1980s upon abundant hydrocarbon exploration data concordantly define an upper stack of nappes, which incorporated since Miocene sedimentary units of the Adria passive margin detached from the original substatum (Figure 1c) [*Mostardini and Merlini*, 1986; *Patacca and Scandone*, 1989; *Casero et al*., 1991; *Mazzoli et al*., 2001]. These units manly include Meso-Cenozoic carbonates of the Apenninic platform and pelagic successions of the Lagonegro basin, stratigraphically covered by Neogene foredeep and satellite basins (Figures 1a–1c) [*Patacca and Scandone*, 2001]. These stacked units migrated eastward, overthrusting the flexed western margin of the AP after late Miocene. The buried Apulian carbonates were in turn involved in the final shortening phases during late Pliocene-early Pleistocene, originating the Inner AP belt (Figure 1c) [*Menardi Noguera and Rea*, 2000]. Subsequent Quaternary extension has been accommodated by a NW-SE trending extensional fault system that postdates and dissects the belt [*Cinque et al*., 1993].

Under the axial part of the range, the Inner AP is structured in major arcs characterized by thrust-related wide antiforms (Figures 1c and 2), with the latter hosting significant hydrocarbon reservoirs [*Shiner et al*., 2004; *Nicolai and Gambini*, 2007]. The carbonate units of the Inner AP are continuous with those of the Outer AP cropping out in the Apulia foreland to the east (Figures 1a–1c) [*Menardi Noguera and Rea*, 2000]. The Outer AP consists of a 6–8 km thick succession of Mezozoic-Tertiary shallow-water/slope carbonates and Triassic evaporites (dolostones with anhydrites), overlying Permo-Triassic clastic deposits (hereafter called Permian basal clastics) [*Roure et al*., 1991]. Sonic logs from deep wells in the foreland provide *P* wave velocities around 6.0 km/s, 6.4 km/s, and 5.5 km/s for Mesozoic-Tertiary limestone, Triassic evaporites, and Permian basal clastics, respectively [*Improta et al*., 2000]. Hence, the Permian basal clastics correspond to a low-velocity layer comprised between the AP and the crystalline continental crust of Apulia. The Outer AP can include basaltic rocks intercalated with Eocene limestone, but location and extension of buried lavas mentioned in *Sella et al*. [1988] are unknown. Mafic lavas and intrusions into the AP were also hypothesized by *Mostardini and Merlini* [1986] based on magnetic positive anomalies of deep origin. However, the only exposures of igneous rocks of the AP are the small intrusions of Punta delle Pietre Nere (hereafter called Pietre Nere) and S. Giovanni in Pane, in the western Gargano promontory (Figure 1a). The former consists of Paleocene alkali melasyenite and melagabbro [*Bigazzi et al*., 1996], the latter of weathered picritic gabbros ascribed to Paleogene [*Moretti et al*., 2011].

While the stack of Apenninic nappes is concordantly interpreted in terms of thin-skinned tectonics, the structural architecture and the tectonic evolution of the AP and underlying crystalline basement are still debated. Opposing thin-skinned (THN) and thick-skinned (THK) tectonic models were proposed and supported by geologic and geophysical data (Figure 1c) [*Roure et al*., 1991; *Menardi Noguera and Rea*, 2000; *Patacca and Scandone*, 2001; *Speranza and Chiappini*, 2002; *Butler et al*., 2004; *Shiner et al*., 2004; *Bisio et al*., 2004; *Scrocca et al*., 2005; *Finetti et al*., 2005; *Improta and Corciulo*, 2006; *Mazzoli et al*., 2008].

This ambiguity mainly derives from the lack of reliable deep seismic constraints. The internal structure of the Apulian axial belt, crucial to sustain one of the two competing tectonic models, is poorly imaged in the CROP-04 profile, the only deep reflection survey in southern Italy [see *Cippitelli*, 2007]. The top of the AP is widely recognized, but its base is imaged only locally in seismic reflection data, including industry lines [*Shiner et al*., 2004]. Hence, structural profiles of the southern Apennines published in recent years present dramatically different THN and THK interpretations of the Apulian carbonate embricates and underlying basement, as well as contrasting estimates of the shortening accumulated by the Inner AP (Figure 1c). Even the THN interpretations of CROP-04 data significantly disagree about the geometry of AP thrusts, Permian basal clastics, and Quaternary extensional faults [see *Scrocca et al*., 2005; *Patacca and Scandone*, 2007; *Cippitelli*, 2007].

Deep seismic interfaces from receiver functions (RFs) do not allow discerning between the two opposite tectonic models but seem to be more consistent with THK interpretations [*Steckler et al*., 2008]. Besides, RFs provide important constraints on the geometry of the Adriatic and Tyrrhenian Moho. The former deepens below the belt from ~30 km in the Apulia foreland to more than 45 km depth in the external Apennines, while the latter is only ~30 km deep under the axial part of the belt and rises to 20–25 km depth under the Tyrrhenian margin [*Piana Agostinetti and Amato*, 2009; *Spada et al*., 2013].

Crustal thinning along the Tyrrhenian margin and regional extension coexists with Quaternary volcanism of the Campanian Province (Figure 1a) [*Peccerillo*, 1999]. Magmatism also took place during middle-late Pleistocene at Mount Vulture volcano that is located in an anomalous eastward position between the outer Apennines and the foreland, external from the geodynamic active front. All these volcanoes are characterized

by both subduction-related and anorogenic intraplate geochemical signatures, with the latter decreasing from Mount Vulture to Neapolitan volcanoes [*De Astis et al*., 2006].

3. Data and Model Inversions

3.1. Inversion Method and Resolution Analysis

The tomographic models presented in this study were determined using the code Simulps14 [*Haslinger*, 1998]. This is an iterative, linearized tomographic technique introduced by *Thurber* [1983] and subsequently modified by *Eberhart-Phillips and Reyners* [1997], in which *P* and *S* arrival times are simultaneously inverted for velocity parameters (*Vp* and *Vp*/*Vs*) and earthquakes location. The velocity model is parameterized by a 3-D grid of nodes with velocity continuously defined through the medium using a linear interpolation between adjacent nodes. Seismic rays are traced using a pseudo-bending method [*Thurber*, 1983], for short distances, and the shooting method [*Virieux and Farra*, 1991] for longer raypaths. The coupling between hypocentral unknowns and velocity parameters is resolved by the parameter separation [*Pavlis and Booker*, 1980]. The final model is obtained by an iterative damped least squares inversion scheme that searches for the best compromise between data misfit reduction and model perturbations. The velocity models and earthquake locations are iteratively upgraded until the variance improvement ceases to be significant, according to an *F* test.

To estimate quantitatively resolution of the velocity models, we performed a complete analysis of the resolution matrix (RM) from which we derived the spread function (SF) and resolution contouring. Each row of RM represents the averaging vector of a generic parameter and contains information on its volumetric estimate. A well-resolved node is characterized by a compact averaging vector with elements close to 1 on the diagonal and to 0 elsewhere. The SF, as defined by *Michelini and McEvilly* [1991], allows to quantify the sharpness of averaging vectors. It is calculated compressing each row of the resolution matrix into a single number that describes how strong and peaked the resolution is for that node [*Toomey and Foulger*, 1989]. The smaller the SF value, the better the resolution for the model parameter.

The classical ways for establishing the threshold of SF above which the resolution of the model is inadequate are (a) the joint analysis of SF and Derivative Weight Sum (DWS) that is a measure of the density of rays around each node [*Toomey and Foulger*, 1989] and (b) the analysis of the directional properties of the parameter estimation (smearing of anomalies) for different SF limits that gives information on the spatial quality of resolution.

For point (a) we reported for each node of the model SF and DWS values in a two-dimensional plot (Figure S1 in the supporting information). Since the resolution is strongly dependent on the quality of sampling, the points define a sort of L-shaped trend, with DWS decreasing as SF gradually increases. Following *Toomey and Foulger* [1989], the threshold of SF is the point where the decrease of DWS is less prominent, and it can be located in the kink of the L-shaped trend. For point (b) we analyzed smearing of anomalies accordingly to *Reyners et al*. [1999] and *Eberhart-Phillips and Chadwick* [2002]. We plot for each node the contour of the 70% of the averaging vector in the RM. If a velocity parameter is well resolved, SF value is small and the 70% contour line encompasses only that node. For a poorly resolved node, SF value increases and the 70% contour line broadens up to enclosing adjacent nodes (see Figures S2 and S3 in the supporting information).

3.2. Graded Inversion Scheme: Application to Southern Apennines and Irpinia Region

Due to the different scale of our target volumes, regional to local, we used a graded inversion approach [*Eberhart-Phillips*, 1993; *Eberhart-Phillips and Reyners*, 1997] to illuminate progressively the crustal structure of southern Apennines with an improved spatial resolution.

First, we used the code Simulps14 to determine a large-scale regional model that includes the southern Apennines and the Apulia foreland (Figure 3). This regional tomography illuminates depths down to 21 km and provides a picture of almost the entire upper crust and midcrust with an inedited spatial resolution. Then, we focused on the Irpinia region, for which we have additional *P* and *S* waves traveltime data provided by the ISNet dense local network (Figure 3) [*Iannaccone et al*., 2010]. For the Irpinia local inversion, we used a finer parameterization and the 3-D regional model as starting model. This graded inversion approach guarantees that deep and long-wavelength regional-scale velocity anomalies are contemporaneously resolved with small-wavelength local-scale features, these later sampled by the local data [*Seccia et al*., 2011].

To choose the optimal parameterization for the regional and Irpinia local models, we run several inversions by using grids with different node spacing. The optimal grid spacing provides the best compromise among

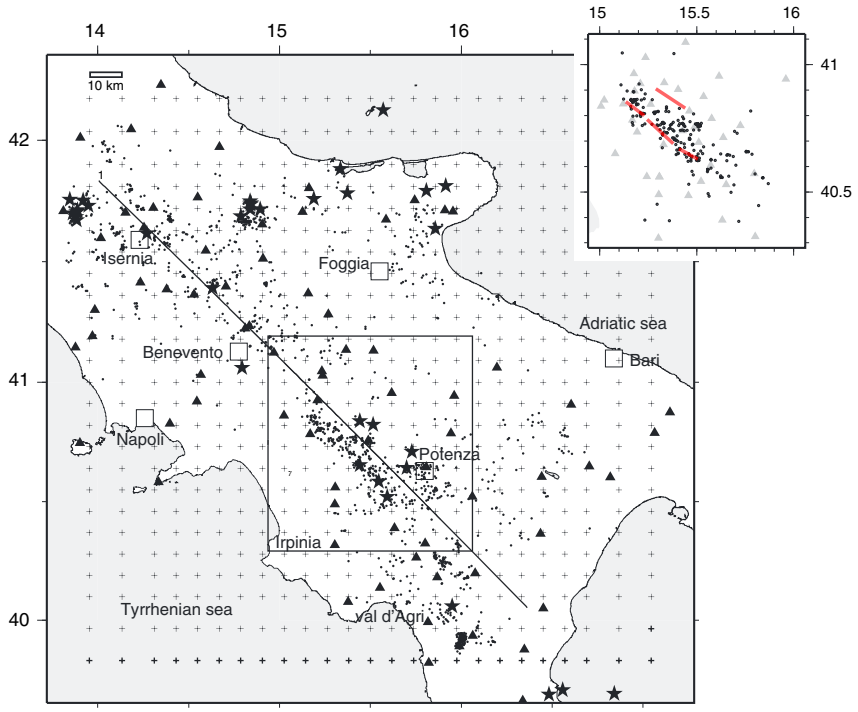

Figure 3. Location of seismic stations (triangles), earthquake (dots), and model nodes (crosses) used in the regional-scale tomographic inversion. Events with $M_L > 4.0$ occurred since 1984 and located by *Chiarabba et al.* [2005] are indicated by stars. The black line is the trace of the velocity section showed in Figure 7. The black squares define boundaries of the Irpinia high-resolution model, with earthquakes and seismic stations of the INGV and ISNet networks reported in the inset map. Thick red lines in the inset map denote fault segments of the 1980 Irpinia earthquake.

data misfit reduction, spatial resolution of the model, and formal resolution of parameters expressed by the RM. The use of a too coarse grid of nodes, with respect to the characteristic wavelength of the velocity anomalies, provides formally well resolved model parameters at the cost of a spatial aliasing of anomalies into the parameter space and of a small reduction of the data misfit [see *Toomey and Foulger*, 1989]. Hence, the shape and location of anomalies can be significantly biased by a wrong parameterization, while the resolution of the parameters is high. On the other hand, the use of a too dense grid of nodes allows overcoming aliasing problems at the cost of a rapid deterioration of parameter resolution in regions of the model not adequately sampled by rays.

The regional and Irpinia models presented in this study are parameterized by a $10 \times 10 \times 3$ km and a $3 \times 3 \times 2$ km grid spacing, respectively. The first parameterization is adequate to image large-wavelength velocity anomalies of the middle crust with a good parameter resolution down to 15 km depth. Also, this grid spacing is adequate to define the largest-scale velocity structures (with horizontal dimension of a few tens of kilometers) of the upper crust. The fine parameterization of the Irpinia model allows imaging the very complex velocity structure of the thrust-and-fold system, which is characterized by wavelength of anomalies of a few kilometers, with a good parameter resolution down to 10 km depth.

3.3. Regional Model

During the past 8 years, the upgrade of the national seismic network managed by INGV has made the investigation of the crustal structure in southern Apennines more feasible. We collected a rich data set of regional to local earthquakes, recorded by a network of up to 80 stations whose spacing is of about 10 km (Figure 3). Arrival times are taken from the Italian Seismic Bulletin released by INGV (available http://bollettinosismico.rm.ingv.it/) that includes handpicked *P*- and *S*-arrival times revised by the analysts of National Earthquake Centre of INGV.

Each phase is weighted on the basis of picking accuracy according to the following scheme: full weight (100%) for reading errors less than 0.05 s, 75% for errors between 0.05 and 0.10 s, 50% for errors between 0.10 and 0.20 s, and 25% for errors between 0.20 and 0.50 s. All the phases with uncertainties greater than 0.5 s have been rejected.

All the seismicity has been preliminarily located using the code Hypoellipse [*Lahr*, 1989]. The 1-D *Vp* model was taken from *Bisio et al*. [2004] that investigated a crustal block corresponding to the northern-central portion of our regional tomographic model (Figure 3). The average *Vp*/*Vs* used in our study, set to 1.83, has been computed using the modified Wadati method [*Chatelain*, 1978]. This relatively high *Vp*/*Vs* value is in agreement with that estimated by local earthquake data for the Lucanian arc (1.83) [see *Maggi et al*., 2009] and the Irpinia region (1.85) [*Matrullo et al*., 2013], and it suggests the presence of highly fractured, fluid-saturated rocks in the upper crust.

Vp values (Table S1 in the supporting information) are consistent with available information on the velocity structure in southern Apennines [*Improta et al*., 2000]. The layers at 0 km (4.3 km/s) and 3 km (5.3 km/s) can be associated to the stack of rootless nappes, which include strongly deformed basin and carbonate platform successions, and to thick Miocene basin sequences of the external Apennines. The layers at 6 km (5.8 km/s), 9 km (6.0 km/s), and 12 km (6.1 km/s) can be related to the 6–8 km thick successions of the Inner and Outer APs. *Vp* values of 6.2 km/s (15 km depth) and 6.5 km/s (18 km depth) can be considered representative of the crystalline continental upper crust and midcrust of Apulia [*Di Stefano et al*., 2009]. The Moho is set to 34 km depth. This value is a representative average of the Moho depths obtained across southern Italy by large-scale tomographic images of the lithosphere [*Di Stefano et al*., 2009] and RF studies [*Piana Agostinetti and Amato*, 2009].

P and *S-P* arrival times from all earthquakes, which satisfy 1-D location hypocentral errors less than 2 km, root-mean-square (RMS) of residuals less than 0.6 s, and azimuthal gap within 180°, were selected for the 3-D regional inversion. These selection criteria ensure a high quality of arrival times and provide an almost homogeneous spatial distribution of seismic rays along the Apenninic belt [see also *Di Stefano et al*., 2009].

The selected data set includes a total of 18,697 *P* wave and 10,795 *S* wave arrival times from 1537 earthquakes occurred from 2006 to 2011, with magnitude ranging from 0.7 to 4.3. The 3-D regional model of the southern Apennines was parameterized with a 10×10 km horizontal node spacing and layers every 3 km depth (Figure 3). After four iterations, the variance reduction is 40% and the final RMS is 0.28 s.

The resolved part of the model, defined on the basis of the criteria described in the subsection 3.1, includes nodes with SF $\leq$2.0. These nodes have compact averaging vectors and 70% smearing contours totally around the respective node (Figure S2). The resolved areas include large part of the inverted nodes in layers at 6, 9, 12, and 15 km depth. Although well-resolved parameters are found down 21 km depth, resolution deteriorates below 15 km depth, especially in the *Vp*/*Vs* model, and is low in the first layer at 3 km depth. The peripheral areas (nodes with $2.0 <$ SF $\leq$2.3) have still a fair resolution but smearing on adjacent nodes is observed. For this reason, we show *Vp* and *Vs*/*Vs* layers from 6 to 15 km depth. The formally well resolved regions (SF $\leq$2.0) in the velocity layers are outlined by continuous lines in Figure 4.

3.4. Irpinia Fine Model

The 3-D regional model was used as starting model in the subsequent higher-resolution tomography aimed at refining the local velocity structure in the Irpinia region (Figure 3). We used a total of 4437 *P* and 3165 *S* wave arrival times from 210 selected earthquakes with local magnitude between 0.6 and 3.2, which were recorded between 2006 and 2010 by 42 seismic stations belonging to the INGV network and to the ISNet local network (Figure 3) (data from ISNet network are available from the Project S5 founded by the Italian Civil Protection Department at http://dpc-s5.rm.ingv.it/it/ScientificReport.html). The 210 earthquakes satisfy the following selection criteria: hypocentral errors less than 1 km, RMS of residuals less than 0.5 s, and azimuthal gap within 180°. Traveltimes were weighted following the scheme reported in subsection 3.3. The Irpinia local model is parameterized by a horizontal grid with a 3×3 km node spacing, and layers are spaced every 2 km depth. After four iterations, the additional variance improvement achieved in the area is 34% and the final RMS is 0.21 s.

The contour of the 70% of the averaging vector of the resolution matrix for each node is shown in Figure S3. The resolved areas of the Irpinia model, defined on the basis of the criteria described in the subsection 3.1, include nodes with SF $\leq$2.3. The resolved nodes are located in the central region that roughly trends NW-SE. Extent of the resolved area strongly decreases below 10 km depth, especially in the *Vp*/*Vs* layers. This lack of resolution in principle precludes the proper imaging of small-scale deep structures, with the exception of a small area in the central part of the model. Anyway, we remind that areas outside the formally well resolved volume of the local model are resolved in the previous regional-scale inversion (Figure S2).

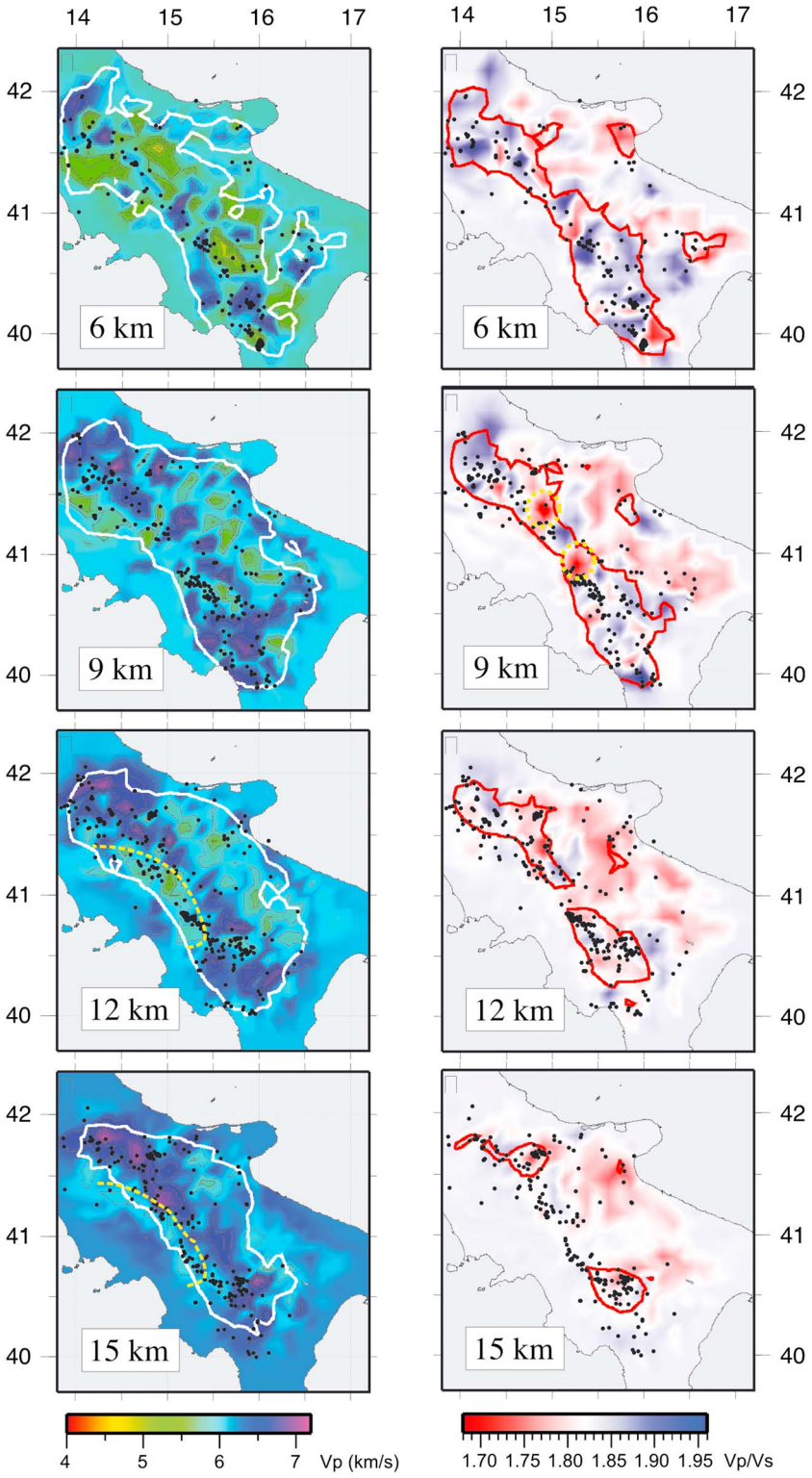

Figure 4. *Vp* and *Vp/Vs* regional models from 6 to 15 km depth. White and red continuous lines enclose the well-resolved volume characterized by nodes with spread function (SF) ≤2.0 (see Figure S2 in the supporting information). Dots denote earthquakes. The dashed yellow line in the layers at 12 and 15 km depth outlines the low-*Vp* region encircling the Neapolitan volcanic district. The two low-*Vp/Vs* spots defined under the axial belt are outlined by yellow dotted circles in the 9 km depth layer.

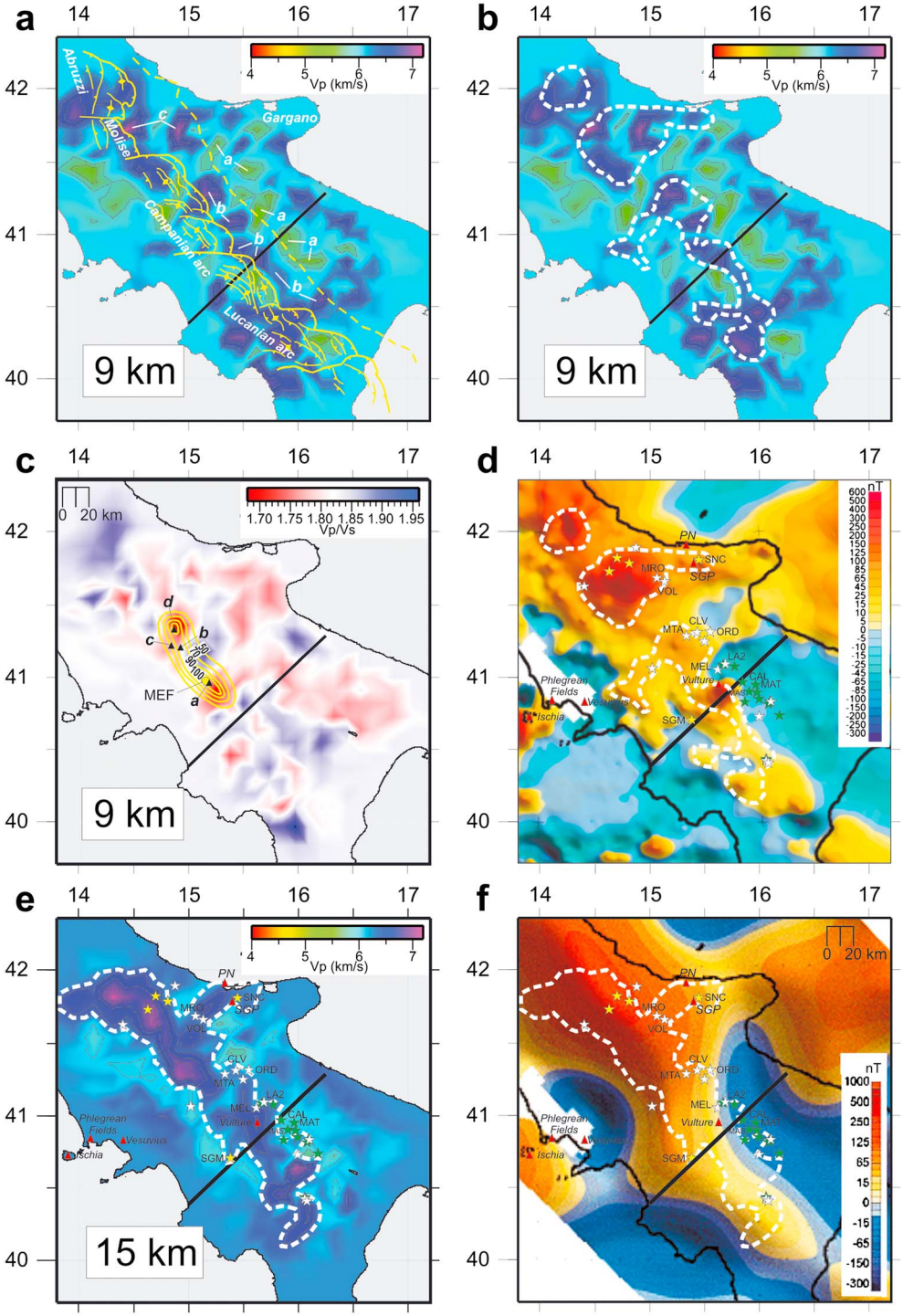

Figure 5

4. Models Description

4.1. Regional Model

Figure 4 shows the *Vp* and *Vp/Vs* values in the inverted layers, revealing the lateral heterogeneity of the sedimentary accretionary prism and of the Apulian crust underneath the mountain range and the foreland. The *P* wave velocity layer at 6 km depth is very heterogeneous (Figure 4), with important lateral variations also along the strike of the belt. These heterogeneities document the extreme structural complexity of the southern Apennines.

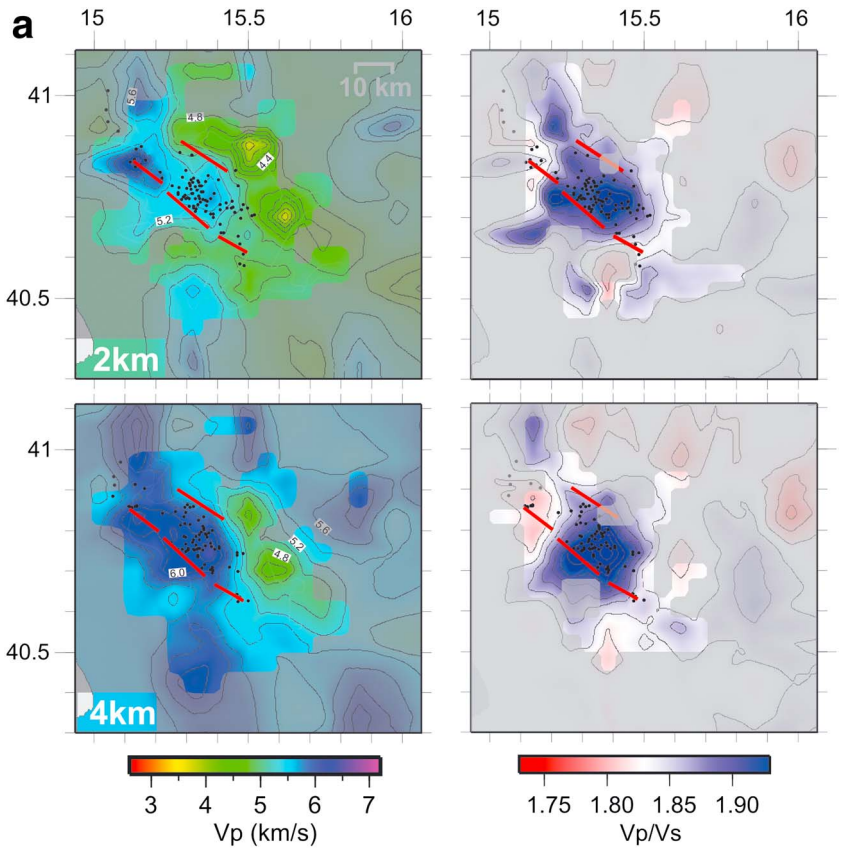

Figure 6. (a) *Vp* and *Vp/Vs* layers of the Irpinia model at 2 and 4 km depth. In the shaded peripheral areas resolution is low (see Figure S3 in the supporting information). Peripheral regions with inadequate resolution (nodes with SF >2.3) are masked by transparency. We remind that these peripheral areas can be resolved in the previous regional-scale inversion (Figure S2). Dots denote earthquakes. Red thick lines outline the fault segments of the 1980 Irpinia earthquake (redrawn from *Pantosti and Valensise* [1990]). (b) *Vp* and *Vp/Vs* layers of the Irpinia model at 6, 8, and 10 km depth. Peripheral region with inadequate resolution (nodes with SF >2.3) is masked by a trasparency. Dots denote earthquakes. Red thick lines outline the fault segments of the 1980 Irpinia earthquake. The yellow star depicts the epicenter of the main shock of the 1980 earthquake.

At 9 km depth, the pattern of *Vp* anomalies shows a prevailing NW-SE trend and the following main features (Figure 5a): (i) a region of negative anomalies (*Vp* around 5.5 km/s) under the Bradanic foredeep to the east of the buried front of the Apennines (see label *a*), (ii) a region of positive anomalies (*Vp* of 6.5–7.0 km/s) under the external Apennines to the east of the buried frontal ramp of the Apulian belt (between about 40.5°N and 41.7°N; see label *b*), (iii) two broad high-*Vp* anomalies (*Vp* up to 7 km/s) at the junction zone between the central and

Figure 5. Comparison of the regional model with structural data and magnetic anomaly maps. (a) Main structural lineaments of the AP are superimposed on the *Vp* layer at 9 km depth. The buried frontal ramp of the AP belt (thick yellow line) and the buried front of the Apennines belt (dashed yellow line) are redrawn from *Nicolai and Gambini* [2007]. Small labels *a* outline low-*Vp* anomalies under the Bradanic foredeep, *b* high-*Vp* anomalies under the external belt, *c* high-*Vp* anomalies under the Abruzzi-Molise boundary. (b) *Vp* layer at 9 km depth with outlined high-velocity regions that have a signature in the magnetic anomaly map shown in Figure 5d. (c) The heat flow anomaly of the axial part of the belt is superimposed on the *Vp/Vs* layer at 9 km depth (isolines are in mW m^{-2}, redrawn from *Italiano et al.* [2000]). Black triangles denote oil wells drilling CO_2 gas caps in the Inner AP (a = Mount Forcuso 1, b = Tranfaglia 1, c = Benevento Sud 1, and d = Benevento 3). The yellow dot depicts the Mefite d'Ansanto degassing site (MEF). (d) Anomaly magnetic map that outlined the anomalies corresponding to high-velocity regions (modified after *Speranza and Chiappini* [2002]). (e) *Vp* layer at 15 km depth that outlined the regional high-velocity anomaly. (f) Low-pass filtered magnetic map (λ = 100 km). The dashed white line defines the extent of the regional anomaly in the 15 km depth layer. Stars denote oil wells that encountered mafic rocks in the AP (yellow = Paleogene intrusions, white = Eocene basalts, and green = Upper Miocene basalts); wells cited in the text are SNC = Sannicandro 1, MRO = Mount Rotaro 2, VOL = Volturino 1, MTA = Mount Taverna 1, CLV = Calvello 1, ORD = Ordona 2, LA2 = Lavello 2, MEL = Melfi 1, CAL = Calvino 1, MAT = Mattinella 1, MAS = Maschito 1, and SGM = San Gregorio Magno 1. Red triangles depict the Paleogene intrusions of Pietre Nere (PN) and S. Giovanni in Pane (SGP) and Quaternary volcanoes. The CROP-04 line is indicated by a thick black line.

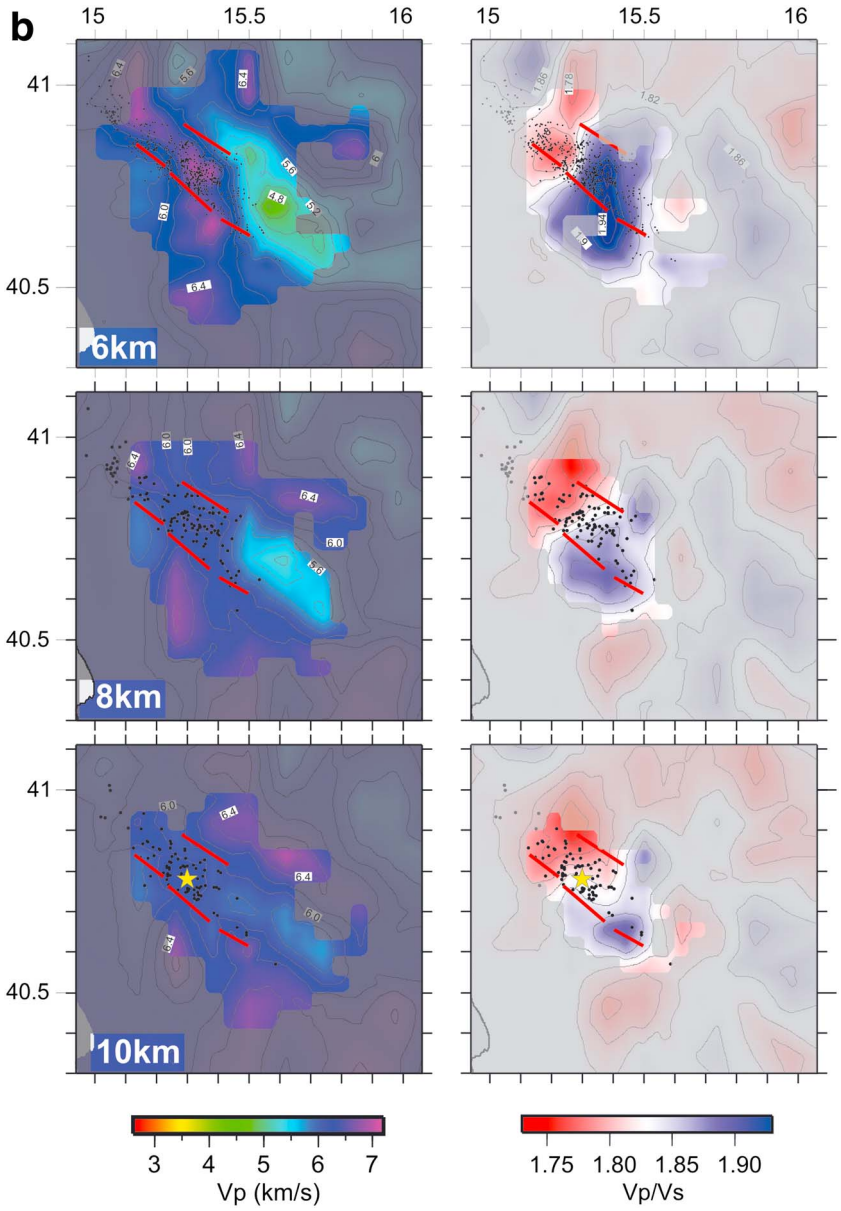

Figure 6. (continued)

southern Apennines (Abruzzi-Molise boundary; see label *c*) and in the southern sector of the belt (Lucanian arc), with the former anomaly that extends to the east toward the Gargano promontory and the latter to the west toward the Tyrrhenian margin. The *P* wave velocity structure is more heterogeneous under the axial zone of the belt (Campanian and Lucanian arcs, between 40.5°N and 41.5°N) that is characterized by a complex pattern of high- and low-*Vp* small anomalies (Figure 5a).

The layer at 15 km depth evidences the vertical and lateral continuity of the high-*Vp* regions defined under the external Apennines and the Abruzzo-Molise boundary (Figure 5e). As a whole, high-*Vp* bodies define a NW-SE trending regional anomaly, with *Vp* of 6.8–7.2 km/s, which extends downward into the midcrust, at least.

A striking decrease of *P* wave velocity ($Vp = 5.5–6.0$ km/s, ΔVp up to −10%) is found at 12–15 km depth in a semicircular area that surrounds the Neapolitan volcanic district, extending from the inner to the axial part of the belt (Figure 4). At 9 km depth, pronounced low-*Vp*/*Vs* volumes are observed on top of this low-velocity anomaly (Figure 4).

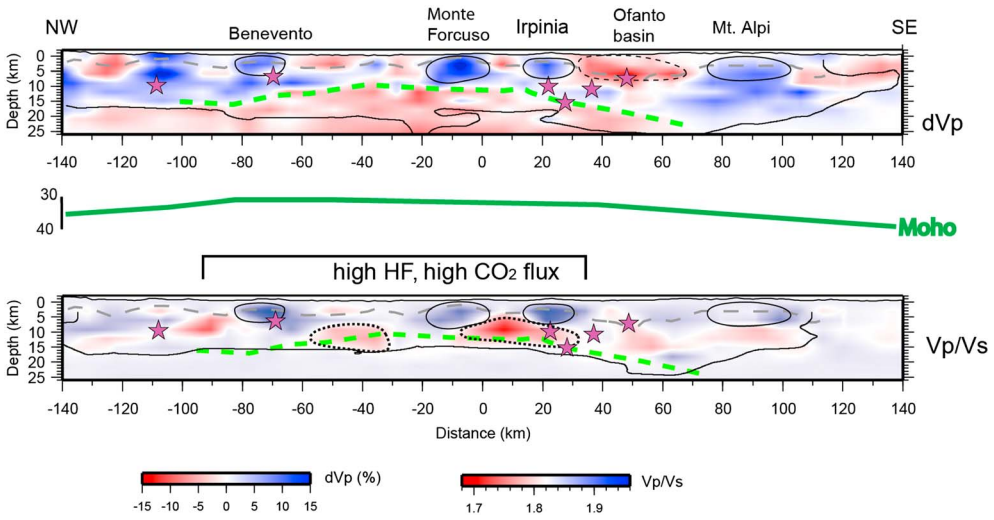

Figure 7. *Vp* perturbation and *Vp/Vs* vertical section along the axial part of the belt, with outlined main anomalies discussed in the text (see the trace of the section in Figure 3). The yellow dashed line bounds the regional *Vp* negative anomaly in the midcrust, black continuous lines are the limits of well-resolved regions characterized by nodes with SF ≤2.0 (see Figure S2 in the supporting information). Purple stars denote $M_L > 4.0$ crustal earthquakes occurred since 1984 [*Chiarabba et al*., 2005] and located within 10 km from the vertical plane. In the data set used for the tomographic inversion, there is only one event with $M_L > 4.0$ located far from the section. High-*Vp* and high-*Vp/Vs* anomalies (outlined by thin black lines) correspond to main structural highs of the Inner AP (Mount Alpi, Irpinia, Monte Forcuso, and Benevento structural trends) [see *Nicolai and Gambini*, 2007]. These anomalies follow main culminations of the top of the AP that is outlined by a dashed gray line in the figure. In the upper crust, pronounced low-*Vp* anomalies correspond to thick stack of nappes including Mesozoic-Tertiary basinal sequences (Ofanto basin). The two low-*Vp/Vs* spots in the midcrust are outlined by dotted circles.

4.2. Irpinia Model

A remarkable feature of the model is a western high-*Vp* region that roughly trends NW-SE beneath the axial zone of the belt (Figure 6). It extends from 2 km (*Vp* up to 5.6 km/s) down to 8 km depth (*Vp* up to 6.6 km/s). High-*Vp/Vs* values (up to 1.95) characterize large part of this anomalous region. This pattern of high-*Vp* and high-*Vp/Vs* anomalies is interrupted at the northwestern edge of the model by a pronounced low-*Vp/Vs* spot defined between 6 and 10 km depth (Figure 6b).

The high-*Vp* region is bounded to the east by a low-*Vp* region that progressively narrows at depth (Figure 6). In the 2–4 km depth layers, it is defined as a continuous stripe that roughly trends NW-SE with *Vp* values of 4.0–4.6 km/s (Figure 6a). At 8 km depth, it is limited to a round-shaped anomaly with *Vp* of 5.2–5.6 km/s (Figure 6b). Between 4 and 6 km depth, the boundary between the two broad regions of high and low velocities corresponds to a strong lateral *Vp* variation (Figures 6a and 6b).

In the external Apennines, two high-*Vp* regions (*Vp* = 6.0–6.4 km/s), with normal to low *Vp/Vs*, are defined at 6 km depth (Figure 6b). The northern one elongates N-S (around 15.5°E), the southern one is round-shaped and bounds to the east the low-velocity central region. The two anomalies merge into a NW-SE trending high-velocity anomaly at 10 km depth, with *Vp* of 6.4–6.6 km/s.

5. Models Interpretation

5.1. Regional Model

Interpretation of the *Vp* and *Vp/Vs* upper layers is based on published structural profiles of the southern Apennines (*Casero et al*. [1991], among others). A NW-SE trending vertical section (Figure 7) helps clarify the interpretation of the complex anomaly pattern found under the axial part of the belt. We distinguish (i) low *Vp*, normal to high *Vp/Vs*, interpreted as thick Meso-Cenozoic sequences of the Lagonegro basin and Neogene foredeep and satellite basins (e.g., Ofanto basin), (ii) high *Vp*, high *Vp/Vs*, related to regional culminations of the Inner AP and interpreted as fractured, water-saturated carbonates (Mount Alpi, Irpinia, Mount Forcuso, and Benevento structural highs of the AP), (iii) high *Vp*, normal to low *Vp/Vs*, interpreted as Apulian crystalline rocks (see section 5.3).

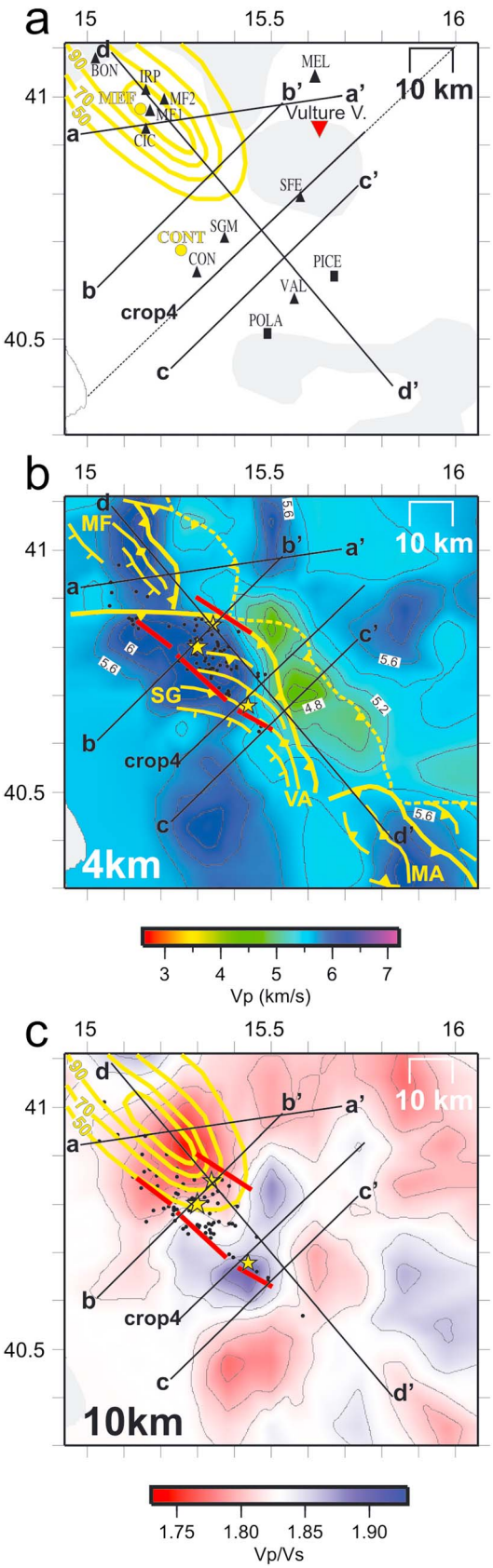

We relate the negative *Vp* anomalies found at 9–12 km depth below the Bradanic foredeep (label *a*, Figure 4) to the low-velocity Permian basal clastics. This interpretation is coherent with magnetotelluric surveys across the Apulia foreland and Bradanic foredeep that reveal the longitudinal continuity of the Permian basal clastics, detected as a conductive layer about 3 km thick [*Patella et al*., 2005]. This layer follows the bending of the Outer AP and is defined at 7–10 km depth under the foredeep. The intense normal faulting of the AP and basement related to the flexural bending of the lithosphere (Figure 1c) could contribute to the decrease of *P* wave velocities.

The low-velocity region observed at 12–15 km depth, encircling the Neapolitan volcanic district (Figure 4), correlates to a pronounced negative anomaly in the uppermost mantle [*Di Stefano et al*., 2009; *Chiarabba and Chiodini*, 2013], a rising of the Moho [*Piana Agostinetti and Amato*, 2009], diffuse CO_2 degassing at the surface [*Chiodini et al*., 2004], and high heat flow [*Mongelli et al*., 1996]. The vertical section in Figure 7 emphasizes the existence of this low-*Vp* zone, we interpret as due to a thermal/fluid anomaly in the crust. This anomaly would originate from the upwelling of the hot asthenospheric mantle wedge that flows from the Tyrrhenian back-arc basin toward and beneath the western part of the Apennines. On top of the low-*Vp* anomaly, two distinct low-*Vp*/*Vs* spots are interpreted as isolated CO_2-rich rock volumes, as discussed in section 5.4.

Figure 8. (a) Traces of the velocity sections and wells shown in Figure 9, with superimposed heat flow anomaly (yellow lines) and main positive magnetic anomalies (gray areas). Wells shown in vertical sections are the following: MF1 = Mount Forcuso 1, MF2 = Mount Forcuso 2, CIC = Ciccone 1, IRP = Irpinia 1, BON = Bonito 1, MEL = Melfi 1, CON = Contursi 1, SGM = San Gregorio Magno 1, SFE = San Fele 1, and VAL = Vallauria 1. The black squares denote stations with RF models. The yellow circles indicate the Mefite d'Ansanto vent (MEF) and the Contursi springs (CONT). (b) The main structural lineaments of the AP are superimposed on the *Vp* layer at 4 km depth, with the main ramp of the Apulian belt indicated by a thicker yellow line (redrawn from *Nicolai and Gambini* [2007]): MF = Mount Forcuso Trend, SG = San Gregorio Trend, VA = Vallauria Trend, and MA = Mount Alpi Trend. (c) The traces of the velocity sections and the heat flow anomaly are superimposed on the *Vp*/*Vs* layer at 10 km depth. The three shocks of the 1980 earthquake (yellow stars) and the ruptured segments (red lines) are showed in Figures 8b and 8c.

5.2. Irpinia Model

The overall pattern of the *Vp* and *Vp/Vs* anomalies under the axial zone of the belt is consistent with previous tomographic models defined through aftershocks data of the 1980 Irpinia earthquake [*Amato et al*., 1992]. With respect to this study, significant improvements of our model are the higher spatial resolution that allows defining fine details of the velocity structure, and the wider extension that allows imaging also the external Apennines.

Interpretation of the velocity structure is constrained by deep oil wells (Figure 8a) and structural maps of the AP featured upon industry reflection profiles [*Nicolai and Gambini*, 2007]. Vertical sections traced across the main arcs of the AP belt and along the CROP-04 profile (Figure 8b) permit to recognize first-order contractional structures (Figures 9 and 10). The geometry of the high-*Vp* broad region in the layer at 4 km depth strictly correlates to main culminations of the Inner AP (Figure 8b). Moreover, the high-velocity pattern is in agreement with the trend of the main Pliocene thrusts and related anticlines in the Apulian carbonates: NNW-SSE trend in the northern arc (Mount Forcuso Trend), WNW-ESE (S. Gregorio Trend) rotating to NNW-SSE (Vallauria Trend) in the central arc, and NW-SE in the southern arc (Mount Alpi Trend) [see, *Nicolai and Gambini*, 2007].

In cross sections, the 5.6–6.0 km/s isovelocity lines follow the top of the AP (Figure 9). Thus, high-*Vp* bumps ($Vp > 5.6$ km/s) correspond to wide ramp anticlines of the Inner AP consisting of Mesozoic fractured limestones. High *Vp/Vs* are indicative of fractured, fluid-saturated carbonates, in agreement with the presence of deep-seated, aqueous reservoirs drilled in the AP. Very high *Vp* spots ($Vp = 6.4$–6.6 km/s) defined around 6 km depth can be related to Triassic evaporitic dolostones in the core of the Apulian anticlines (Figures 9 and 10).

Low-*Vp* regions ($Vp = 5.8$–6.0 km/s) are defined under the Triassic evaporites (Figures 9 and 10). The velocity reduction can be related to the Permian basal clastics that are imaged locally under the Inner AP in the Lucanian arc [*Shiner et al*., 2004]. This finding is consistent with RF inversion for station POLA [*Steckler et al*., 2008]: a low-*Vs* layer resolved at about 10 km depth was interpreted as the Permian basal clastics comprised between the Apulian carbonate multilayer and the crystalline upper crust (Figure 9c).

The low-*Vp* broad region defined in the central part of the model coincides with the abrupt deepening of the AP to the east of the buried frontal ramp of the Apulian belt (Figure 8b). Low-*Vp* bodies ($Vp = 3.8$–5.0 km/s) correspond to a thick stack of Meso-Cenozoic basinal units (S. Fele antiform; see map in Figure 1a and sections in Figures 9c and 10) and to Pliocene satellite basins (Trevico and Ofanto basins; see map in Figure 1a and sections in Figures 9a and 9b).

The *Vp* structure under the external Apennines is in general agreement with the northeastern rise of the Outer AP (Figures 9a–9c). However, we do not relate the very high *Vp* bodies ($Vp = 6.4$–6.6 km/s) defined below 4–6 km depth to the Apulian carbonates, as discussed in the next paragraph.

The pattern of high- and low-*Vp* regions of the Irpinia model is in close agreement with recently published results by *Amoroso et al*. [2014]. Nevertheless, the two models differ significantly in absolute values of *Vp* in the broad high-*Vp* region in the western sector. *Vp* values larger than 6.0 km/s are found beneath 6 km or 3–4 km depth in the model of *Amoroso et al*. [2014] and in our model, respectively. Hence, according to *Amoroso et al*. [2014], the top of the AP corresponds the isovelocity curves of 4–4.5 km/s, while *Vp* increases up 5.5–6 km/s between 8 and 12 km depth. In our model, isovelocity curves of 5.6–6.0 km/s follow the top of the AP that is 3–4 km deep along the S.Gregorio Trend [*Nicolai and Gambini*, 2007]. Our results are in better agreement with subsurface constraints because sonic logs from wells penetrating the S. Gregorio Trend [see *Amoroso et al*., 2014, Figure 2b] and the Mount Forcuso Trend [*Improta et al*., 2003a] show the Apulian limestones with *Vp* around 6.0 km/s.

The high-*Vp/Vs* body found in the western sector of our model in correspondence of the S. Gregorio Trend (Figures 6a, 6b, and 9b–9c) is consistent with a strong anomaly defined by *Amoroso et al*. [2014]. The authors relate very high *Vp/Vs* values (up to 2.2) to a fault-bounded block consisting of fractured and water-saturated Apulian carbonates with high pore fluid pressure. Conversely, in *Amoroso et al*. [2014] there is no indication of the deep low-*Vp/Vs* body resolved at the northwestern edge of our model below the AP (Figures 6a, 6b, and 6d). Likely, this depends on the different inversion approach used in our study that combines regional and local earthquake data in a graded inversion scheme, and in *Amoroso et al*. [2014] that uses only local data.

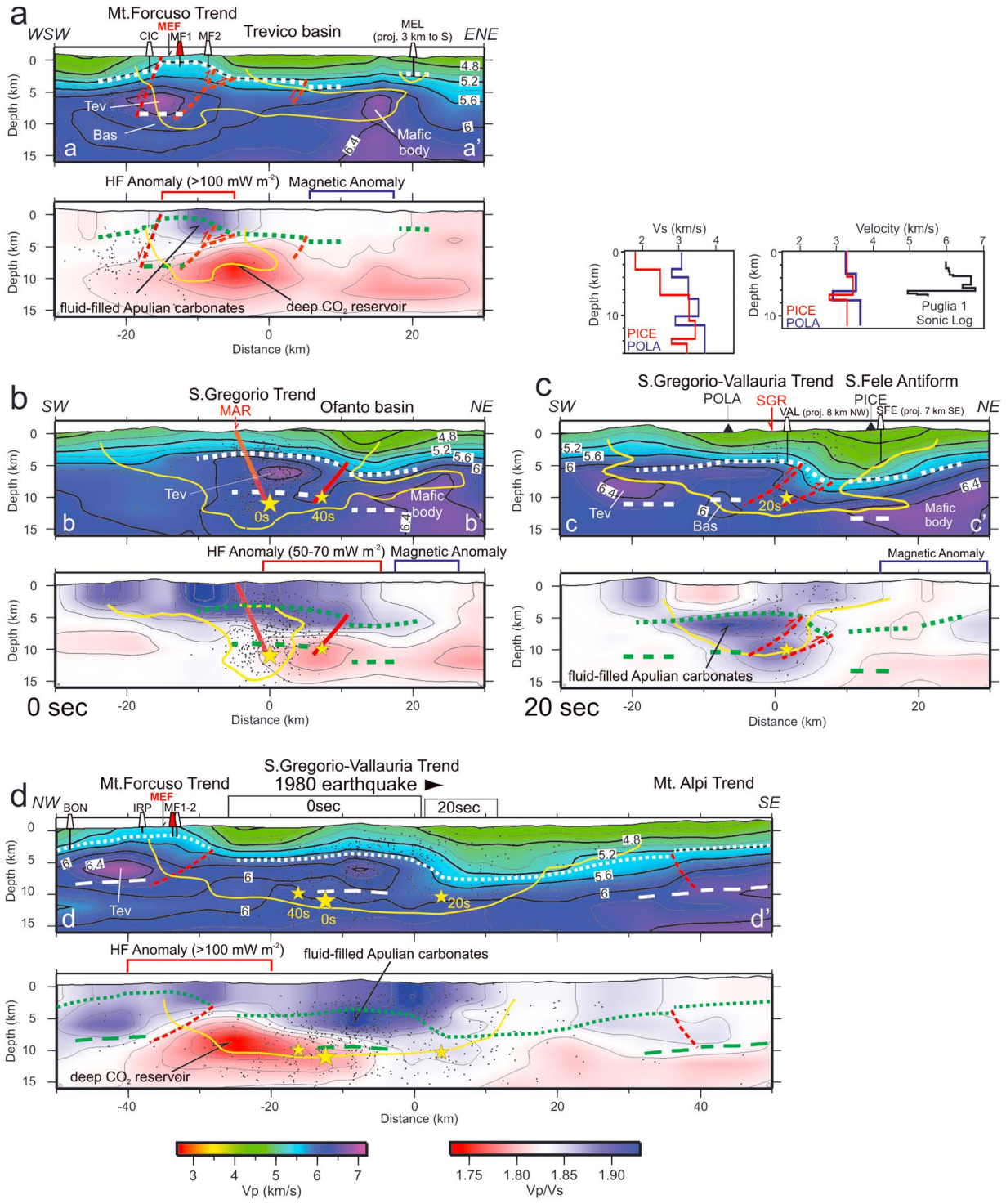

Figure 9. (a–d) *Vp* and *Vp/Vs* vertical sections of the Irpinia model. The well-resolved area (SF ≤ 2.3) is contoured in yellow. We remind that the velocities outside this area are resolved in the regional model. White and green dotted lines indicate the top of the AP (modified after *Nicolai and Gambini* [2007]), while white and green dashed lines indicate the presumed base of the AP (Tev = high-velocity Triassic dolostones and Bas = low-velocity Permian basal clastics). The main faults of the AP constrained by industry reflection data are outlined by red dashed lines. Section C-C′ is complemented by RF models for stations POLA and PICE (black triangles) that constrain the depth of the Permian basal clastics (modified after *Steckler et al.* [2008]): the plot on the left shows the *Vs*-depth profiles, the plot on the right the *Vs* profiles from the top of the AP and the sonic log of the Puglia 1 well that reaches the basal clastics in the Apulian foreland. Oil wells are CIC = Ciccone 1, MF1 = Mount Forcuso 1 (outlined in red), MF2 = Mount Forcuso 2, MEL = Melfi 1, IRP = Irpinia 1, BON = Bonito 1, VAL = Vallauria 1, and SFE = San Fele 1. The Mefite d'Ansanto (MEF) is reported in sections *a* and *d*. Sections *b* and *c* cross the fault segments of the 1980 Irpinia earthquake (thick red lines), while section *d* runs along the collapsed hanging wall block. The yellow stars denote the three shocks, the red arrows fault scarps of Mount Marzano (MAR) and S. Gregorio (SGR).

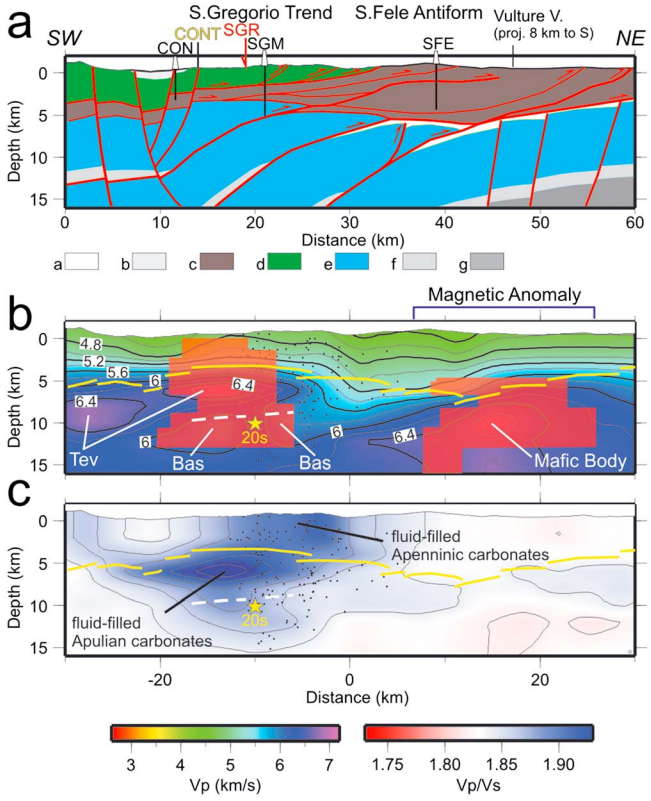

Figure 10. *Vp* and *Vp/Vs* vertical sections along the CROP-04 line. (a) Interpretation of the CROP profile modified after *Scrocca et al.* [2005]: a = Plio-Pleistocene deposits, b = Internal nappes, c = Meso-Cenozoic basinal units, d = Apenninic carbonate platform, e = AP, f = Permo-Triassic basal clastics, and g = Apulia upper crust. Oil wells are CON = Contursi 1, SGM = San Gregorio Magno 1, and SFE = San Fele 1. The 1980 S. Gregorio fault scarp (SGR) and the Contursi hot springs (CONT) are shown. (b) *Vp* section with superimposed the top of the AP redrawn from *Scrocca et al.* [2005] (yellow lines), the presumed base of the AP (dashed white line) and the 20 s shock of the Irpinia earthquake (yellow star). The red transparencies correspond to the low-resistivity bodies of *Patella et al.* [2005]. (c) *Vp/Vs* vertical section.

5.3. The Nature of the High-*Vp* Anomalies in the Apulian Upper-Middle Crusts

Remarkable high-*Vp* anomalies in the upper crust and midcrust are observed from the Abruzzi-Molise boundary to the western Gargano promontory and along the external Apennines (Figures 5a and 5e). These high-*Vp* bodies correlate with first-order positive magnetic anomalies [*Speranza and Chiappini*, 2002; *Caratori Tontini et al.*, 2004]. High-*Vp* regions at 9 km depth correlate to a broad magnetic anomaly (exceeding 100 nT) that extends from the Abruzzi-Molise region to the Gargano promontory, and with smaller positive anomalies (40–80 nT) distributed along the external Apennines and to the south of Mount Vulture (Figures 5b and 5d). This correlation is stronger by comparing high-*Vp* anomalies at 15 km depth with low-pass filtered positive magnetic anomalies (Figures 5e and 5f). In *Speranza and Chiappini* [2002], the source of the strong anomaly in the Abruzzi-Molise region is estimated at depths ranging between 13 and 18 km, a range consistent with that of the high-*Vp* body. This points to a common source of the magnetic and velocity anomalies.

Speranza and Chiappini [2002] propose as possible source of magnetic anomalies either a differentiated lower Apulian basement contaminated by mafic intrusions or an heterogeneous Apulian basement, preferring the latter interpretation because of the regular pattern of the anomaly along the belt and the parallelism with the thrust fronts. Their model consists of a composite magnetic basement wedge ramping over the Apulian basement. The wedge incorporates two highly susceptibility thrust sheets of lower crust upthrown under the external and axial parts of the Apennines, in agreement with a thick-skinned tectonic evolution of the Apulian belt.

We interpret these external high-velocity bodies, which relate to strong magnetic anomalies of deep origin, as due to mafic intrusions into the upper crust and midcrust. In accordance, *Patacca* [2007] and *Cippitelli* [2007] reported mafic intrusions or volcanites, Eocenic to Miocenic in age, drilled by some oil wells in both the Outer AP (Mattinella 1, Maschito 1, and Calvino 1 wells) and Inner AP (San Gregorio Magno 1 well) (Figure 5d). However, a specific study of well data aimed at recognizing igneous rocks of the AP is still lacking.

In order to assess how diffuse are Cenozoic mafic rocks in the AP and how spatially they relate to the high-*Vp* anomalies, we performed an extensive analysis of oil wells drilled in southern Italy (available from the ViDEPI Project at http://unmig.sviluppoeconomico.gov.it/videpi/pozzi/pozzi.asp). We analyzed and interpreted stratigraphic data and logs from more than 160 wells penetrating the AP. Our analysis allowed the identification of 33 wells that encountered mafic rocks in the upper portion of the AP (Figure 5d). These wells

were grouped in three classes based on the encountered rocks: (A) Paleogene mafic intrusions, (B) Eocene basaltic lavas, and (C) Upper Miocene basaltic lavas and tuffs (see Table S2 in the supporting information for more details).

1. In the Abruzzi-Molise boundary, four wells penetrated repeated mafic intrusions, up to 30 m thick, in Mesozoic carbonates between 2500 and 4000 m depth (yellow stars in Figure 5d). All wells fall within the round-shaped intense magnetic anomaly (Figure 5d) and high-*Vp* regions (Figure 5b). Well Sannicandro 1, in the western Gargano promontory, is a few kilometers apart from the small intrusions of Pietre Nere and S. Giovanni in Pane (Figure 5d). The well and the both mafic outcrops match the eastward extension of the velocity/magnetic anomaly that roughly trends W-E (Figures 5b and 5d–5f).
   Just in this area, *Loddo et al*. [1996] modeled gravimetric and magnetic anomalies revealed by high-resolution surveys as due to a wide, ramified mafic intrusion into the Apulian carbonates and basement. Farther south, in the belt axial zone, the San Gregorio Magno 1 well (Figure 5d) encountered eight Paleocene-Eocene gabbroic dykes, up to 40 m thick, in Jurassic carbonates between 5090 and 5848 m depth. This borehole is located in correspondence of the southern prolongation of the long-wavelength magnetic positive anomaly (Figure 5f).
2. Several wells located between the Bradanic foredeep and the axial zone of the belt encountered layers of basalt in Eocene breccia limestones or calcareous slope breccias with abundant clasts of basalt. The Eocene basalts are distributed along 150 km of the southern Apennines (white stars in Figure 5d). In some wells (Calvello 1, Ordona 2, and Lavello 2, outlined in Figure 5d) the carbonates with basalt intercalations are covered by a basaltic layer, 120 m to 150 m thick (see Table S2). This layer is in turn overlaid unconformable red clays of Miocene that document emersion and intense erosion of the underlying basalts. We observe that wells penetrating Eocene basalts are mostly located in correspondence of positive anomalies (Figure 5d). However, some velocity/magnetic anomalies located in the external Apennines (around 41.25°N and 15.25°E) and to the south of Mount Vulture remain unsampled due to the absence of deep wells reaching the AP.
3. Basaltic tuffs intercalated with upper Miocene sediments were reported by *Cippitelli* [2007] for the Calvino 1 well (Figure 5d). Our analysis reveals for the first time that upper Miocene basic vulcanites are widespread along a 60 km long sector of the AP buried under the Bradanic foredeep (green stars in Figure 5d). In this sector, that had been affected previously by basalt extrusions during Eocene, wells encountered basalt or tuff, up to 20 m thick, intercalated with shallow-water carbonates and red clays of Tortonian age. These sequences rest unconformably on Eocene or Cretaceous limestone and sometimes include bauxite deposits (Maschito 1 and Banzi 1 wells) or red paleosols (Calvino 1 well). The presence of laterites and paleosols indicates that the upper Miocene volcanism was coeval to episodes of emersion of the AP.

All these new evidences support our interpretation of the velocity/magnetic positive anomalies in the external Apennines (labels *b* and *c* in Figure 5a) in terms of large mafic bodies intruded into the upper crust and midcrust of Apulia. High-*Vp* intrusions (*Vp* = 6.4–6.6 km/s) are embedded from 5 to 15 km depth (at least) in the Apulian carbonates and basement (Figures 9a–9c and 10), which exhibit lower velocities (*Vp* around 6.0 km/s). According to this interpretation, the basic rocks drilled in the AP represent the shallow manifestations of Cenozoic magmatic episodes [*Lustrino and Wilson*, 2007] that produced these large, deep intrusions. A mafic "gabbroic" nature of the intrusions is in agreement with (i) high velocities around 6.5–6.7 km/s [*Mackenzie et al*., 2005; *Sandrin and Thybo*, 2008], (ii) the occurrence in nearby wells of very thick Eocene basaltic lavas intercalated with Apulian carbonates (Melfi 1 well, Figure 9a), and (iii) the petrology of Pietre Nere igneous rocks in western Gargano [*Bigazzi et al*., 1996].

5.4. The Nature of Midcrustal Low-*Vp* and Low-*Vp*/*Vs* Anomalies in the Campanian Apennines

The inner and axial part of the mountain belt has a pronounced negative anomaly (ΔVp up to -10%) in the midcrust (Figures 5 and 7) that we interpret as a thermal/fluid anomaly caused by the upwelling of the hot Tyrrhenian mantle wedge beneath the Apennines [*Chiarabba and Chiodini*, 2013]. On top of this regional anomaly, two negative *Vp*/*Vs* spots are defined at 9 km depth. The southern one is very clear in the Irpinia model at 8–10 km depth (Figure 6b). In cross sections, it is defined as a dome-shaped body, 20 km long and 15 km wide, with the base at 10–11 km depth and the top at 6–7 km, underneath the wide anticline of Mount Forcuso (Figures 9a and 9d). This anomalous body, with *Vp*/*Vs* as low as 1.75, coincides with a weak low-*Vp* anomaly (*Vp* = 5.8–6.0 km/s).

We interpret the low-*Vp*/*Vs* spots as pressurized CO_2-rich rock volumes developed just below the AP and fed by fluid-rich mantle melts intruded into the crust (e.g., the midcrustal, regional low-*Vp* anomaly). This interpretation relies on published heat flow and geochemical studies, complemented by our analysis of hydrocarbon exploration data. The two low-*Vp* and low-*Vp*/*Vs* regions strictly correlate to the most important heat flow anomaly in the southern Apennines (Figure 5c) [*Mongelli et al*., 1996]. This anomaly extends for 80 km along the axial zone of the belt and was related by *Della Vedova et al*. [2001] to the up flow of warm waters through structural highs of the AP.

The highest-heat flow values (100–215 mW m^{-2}) are observed southward along the Mount Forcuso antiform (Figures 8a, 8b, 9a, and 9d). Here anomalous thermal gradients were recorded in shallow boreholes [*Mongelli et al*., 1996] and oil wells [*Della Vedova et al*., 2001]. Just in this area, the Mefite d'Ansanto degassing site (Figure 8a) is characterized by a huge nonvolcanic CO_2-rich emission, likely the largest in the world [*Italiano et al*., 2000; *Chiodini et al*., 2010]. Geochemical data indicate a deep, mantle-related source of the emitted fluids. In *Chiodini et al*. [2010], Mefite d'Ansanto is fed by an overpressurized CO_2 reservoir of the AP that is in turn recharged by deep mantle fluids. This interpretation is constrained by the nearby Mount Forcuso 1 well that encountered between 1128 and 1600 m depth an overpressurized CO_2 gas cap of a deep-seated aqueous reservoir in Apulian fractured limestone.

The aqueous, fractured reservoir drilled under the Mount Forcuso antiform has a clear signature in the Irpinia model, specifically the high-*Vp* anticlinal structure with very high *Vp*/*Vs* (Figures 9a and 9d). Clearly, the gas cap is beyond the resolution limits of our velocity model. We remark that the low *Vp*, very low *Vp*/*Vs* dome-shaped body develops beneath the Mount Forcuso antiform, which is characterized by the highest-heat flow values ($>$100 mW m^{-2}), the Mefite d'Ansanto degassing site, and the shallow overpressurized CO_2 gas cap drilled by the Mount Forcuso 1 well (Figure 8). This correspondence strongly supports the interpretation of the deep, low-*Vp*/*Vs* body as a pressurized CO_2 rock volume.

In addition to Mount Forcuso 1, we find other three wells that encountered oil/aqueous Apulian reservoirs with gas caps of pressurized CO_2 (Tranfaglia 1, Benevento Sud 1, and Benevento 3 wells, available from the ViDEPI Project at http://unmig.sviluppoeconomico.gov.it/videpi/pozzi/pozzi.asp). All three oil wells fall inside the high heat flow area, in correspondence of the northern low-*Vp*/*Vs* anomaly (Figure 5c). Additionally, they fall inside the eastern sector of the Campanian Degassing Structure [*Chiodini et al*., 2004]. These findings again point to the occurrence of deep, pressurized CO_2 rock volumes that in turn fed minor gas caps confined by structural traps at the top of the Inner AP.

6. The Velocity Structure Along the CROP-04 Seismic Profile

A comparison between the CROP-04 profile and our velocity sections is complicated because significantly different seismic interpretations of the Apulian structures exit [*Scrocca et al*., 2005, 2007; *Patacca and Scandone*, 2007; *Cippitelli*, 2007]. In Figure 10 the *Vp* and *Vp*/*Vs* sections are compared to the thin-skinned model of *Scrocca et al*. [2005]. We selected this model because (i) *Scrocca et al*. [2005, 2007] provided both the interpreted two-way times stack section and the depth-converted model and (ii) among the published interpretations, the top of the AP is in better agreement with the trend of 5.6–6.0 km/s isovelocity lines in the tomographic section.

6.1. Inferences on Tectonic Style of Southern Apennines

We find an overall consistency between the 5.6–6.0 km/s isovelocity lines and the top of AP in the western and eastern sectors, and an evident discrepancy in the central one where the *Vp* model suggests a deeper AP (Figure 10b). Here the 5.6–6.0 km/s contours abruptly deepen to the east of the S. Gregorio Trend in correspondence of a strong lateral *Vp* variation. This feature is more consistent with a deeply rooted high-angle ramp, which upthrow the Inner AP and basement, rather than with long, low-angle thrusts (see section A-A′ in Figure 1c). The latter should cause a smooth geometry of the top of AP and a significant thickening of the stacked carbonate sequences (see section B-B′ in Figure 1c), features not evident in the tomographic section. In addition, the thick low-*Vp* layer of Permian basal clastics, that is not evident in *Scrocca et al*. [2005, 2007], fits better with the existence of deeply rooted, high-angle thrusts at the eastern edge of the S. Gregorio Trend. Our conclusions are also coherent with RF for stations POLA and PICE [*Steckler et al*., 2008], which are located southward, in the hanging wall and footwall of the frontal ramp of the AP belt, respectively

(Figures 8a and 8b). Under the rootless nappes, the *Vs* layering is almost identical to that observed at stations located in the foreland, which are firmly constrained by deep wells penetrating the base of the AP (Figure 9c). Thus, RF inversion concordantly resolve a low-*Vs* layer corresponding to the Permian basal clastics, without an evident thickening of the AP carbonate multilayer under the axial belt (e.g., POLA station), in agreement with THK-tectonic models of the Inner AP (section A-A' in Figure 1c).

6.2. Inferences on Cenozoic Mafic Intrusions

The CROP-04 profile runs above a large mafic body hypothesized under the external Apennines, to the south of Mount Vulture (Figure 10b). This body, we relate to Cenozoic intraplate magmatism, is revealed by the concurrence of a strong high-velocity anomaly (Figure 6b) and of a magnetic anomaly of deep origin (Figure 5d) [*Anelli et al*., 2007]. In the CROP interpretations, no structures or features referable to magmatic intrusions are identified under the belt [*Scrocca et al*., 2005, 2007; *Patacca and Scandone*, 2007; *Cippitelli*, 2007]. The absence of such features both in CROP and in industry seismic lines can be explained by the poor quality of reflection imaging below the top of the AP [*Shiner et al*., 2004; *Cippitelli*, 2007]. Additionally, large intrusions are commonly characterized by a gradual internal velocity increase with depth, with no internal layering causative of strong reflections [*Thybo and Nielsen*, 2012]. Anyway, the existence of a large mafic body under the seismic line is also supported by magnetotelluric surveys carried out in the framework of the CROP-04 project [*Patella et al*., 2005]. The high-velocity region coincides with a low-resistivity body identified inside the highly resistive AP and basement from 5 km to 15 km depth, at least (Figure 10b). We remind that this high-*Vp* region, associated to low-resistivity/magnetic rocks, roots into the regional high-velocity anomaly defined in the midcrust (Figure 5e).

6.3. Clues to Support Deep Fluids Circulation Along the Fault System

Patella et al. [2005] also identify a very low resistivity region (with values as low as 3 Ωm) under the western portion of the CROP-04 line (Figure 10b). This region cuts both the rootless nappes and the AP, includes low- and high-velocity rock volumes, and does not have an evident signature in the magnetic anomaly map (Figure 5d). All these points are in contrast with an interpretation in terms of a large, Paleogene mafic intrusion, even if we can rule out that localized high-*Vp* spot in the Inner AP (Figure 10b) might represent the signature of dolomites with localized gabbroic intrusions, as those drilled in the well S. Gregorio Magno 1 [*Patacca*, 2007].

Alternatively, we interpret the highly conductive region as a weakness zone associated with large Quaternary normal faults and high-pressure fluids, likely of deep origin. This interpretation is supported by several lines of evidence (Figure 10): (i) the CROP data that define deeply rooted Quaternary normal faults [*Scrocca et al*., 2005; *Cippitelli*, 2007], (ii) the coincidence with the source of the 1980 Irpinia earthquake, (iii) high *Vp*, high *Vp*/*Vs* indicative of fractured, fluid-saturated rock volumes, (iv) recent geochemical analysis along the surface ruptures of the 1980 earthquake that provide evidence of migration of deep-seated fluids along the fault segments [*Ciotoli et al*., 2014], and (v) the coincidence with the Contursi hot springs showing deep, mantle-related geochemical signatures [*Italiano et al*., 2000].

Additionally, the upraising of deep, hot fluids is consistent with the low-velocity (thermal/fluid) anomaly defined in the regional model at 12–15 km depth (around 40.6°N and 15.2°E; Figure 4).

7. Discussion

The integration of tomographic images with subsurface constraints from hydrocarbon exploration and the comparison with published magnetic, heat flow, magnetotelluric data have led to a more complete comprehension of the crustal structure in southern Apennines. This has wide implications for a better understanding of the Cenozoic magmatism and tectonic evolution of the Apulian domain, as well as of the CO_2 degassing and seismogenesis in southern Apennines.

7.1. Inferences on the Cenozoic Anorogenic Magmatism

The reconnaissance of high-velocity, high-susceptibility large mafic intrusions in the midcrust/upper crust of southern Apennines opens a new perspective for understanding the Cenozoic anorogenic intraplate magmatism developed within the circum-Mediterranean region [*Lustrino and Wilson*, 2007]. Our results indicate that the Paleogene anorogenic volcanism of Apulia was not a local phenomena

restricted to the small intrusion of Pietre Nere [*Bianchini et al*., 2008], but interested a broad sector of the Apulo-Adriatic domain, probably extending northward up to the Veneto Volcanic Province in eastern Alps [*Macera et al*., 2003].

According to recent studies, a common sublithospheric source exists for the Paleogene magmatism. It has been differently related to (i) adiabatic upwelling of asthenospheric mantle in response to lithospheric extension [*Lustrino and Wilson*, 2007], (ii) active upwelling of lower mantle plumes [*Bianchini et al*., 2008], and (iii) fossilized mantle-plume head trapped beneath the lithosphere [*Piromallo et al*., 2008].

The location and geometry of the emplaced mafic bodies, revealed by our study, indicate that Paleocene-Eocene magmatism was presumably controlled by zones of weakness in the crust, related to an extensional phase that developed along the western margin of the Apulian domain [*Sella et al*., 1988; *Cippitelli*, 2007]. The link between magmatism and extensional tectonics is also suggested by several oil wells in the Bradanic foredeep that encountered Eocene basalts intercalated with slope to pelagic sequences documenting drowning of the AP (wells Mount Rotaro 2, Volturino 1, Mount Taverna 1, Lavello 2, and Melfi 1, outlined in Figure 5d). Extension is also documented on faults exposed in the Apennines, although the role of Paleogene extensional tectonics is still underestimated [*Bigi and Costa Pisani*, 2005, and references therein]. This concomitance suggests that the anorogenic magmatism of the Apulian domain is more consistent with a passive upwelling of asthenospheric mantle due to adiabatic decompression in response to lithosphere extension [*Lustrino and Wilson*, 2007]. Based on *P* wave anomalies in the upper mantle, *Giacomuzzi et al*. [2011] recently proposed that the Adriatic lithosphere sustained an episode of hydration and thinning during the Alpine subduction, related to extension of the crust. Our results support and extend with independent observations this idea to a broad part of the Adriatic plate.

As a smaller part of the Cenozoic anorogenic magmatism, the origin of the widespread upper Miocene basic volcanics, recognized for the first time in this study through well data, is unclear. Magmatism took place in a sector of the Apulia foreland previously affected by the Eocene episode, and later buried beneath the Pliocene foredeep and external thrusts (Figures 5a and 5d). The proximity with Mount Vulture is striking (Figure 5d). Mount Vulture erupted during Pleistocene basic magmas originated by mantle sources with both subduction-related and anorogenic intraplate geochemical features [*Beccaluva et al*., 2002]. This peculiarity is ascribed to the inflow of orogenic-subduction components (k-metasomatism) to an intraplate mantle source during the opening of a slab tear in the eastward retreating Apulian lithosphere [*Lucente et al*., 2006; *De Astis et al*., 2006; *Bianchini et al*., 2008; *Giacomuzzi et al*., 2012]. The intrusion and ascent of the mantle melts would have been promoted by NW-SE lithospheric extensional faults [see *Beccaluva et al*., 2002]. This hypothesis fits well with the presence of the high-velocity crustal anomaly that trends NW-SE under the volcano (Figure 5e).

Summarizing, a broad weakness zone developed during Paleocene-Eocene in the Adriatic lithosphere (e.g., Apulian domain), influencing three episodes of basic magmatism. The Paleocene-Eocene episode, and presumably the Miocene one, can be ascribed to anorogenic intraplate activity promoted by extensional tectonic phases. The Pleistocene magmatism of Mount Vulture can be related to "hybrid" mantle melts that rose up along the preexisting weakness zone of the Adriatic plate actually buried under the external Apennines. This idea supports the model of *De Astis et al*. [2006] that relates the strong intraplate signature of Mount Vulture to melts originated from asthenospheric mantle beneath the Adriatic plate.

7.2. Methodological Implications on the Definition of Tectonic Models of the Southern Apennines

This study has important implication for the use of crustal velocity models or magnetic data to constrain the tectonic style of southern Apennines (e.g., THN- or THK-tectonic models). We showed that the broad high-*Vp* anomalies defined in the upper crust-midcrust can be reasonably interpreted as large intrusive bodies. Although we cannot rule out that high-*Vp* spots identified under culminations of the Inner AP may represent slices of crystalline rocks [*Valoroso et al*., 2011], we suggest that great caution should be used in interpreting high *Vp* or highly susceptibility bodies under the AP as evidence for huge basement thrusts involved in the belt during THK tectonics [*Chiarabba and Amato*, 1997; *Speranza and Chiappini*, 2002; *Bisio et al*., 2004; *Improta and Corciulo*, 2006]. Nevertheless, the velocity structure of the axial part of the range, along the CROP-04 line, is better explained by deeply rooted high-angle thrusts, in agreement with a THK tectonic evolution of the Pliocene Apulian belt.

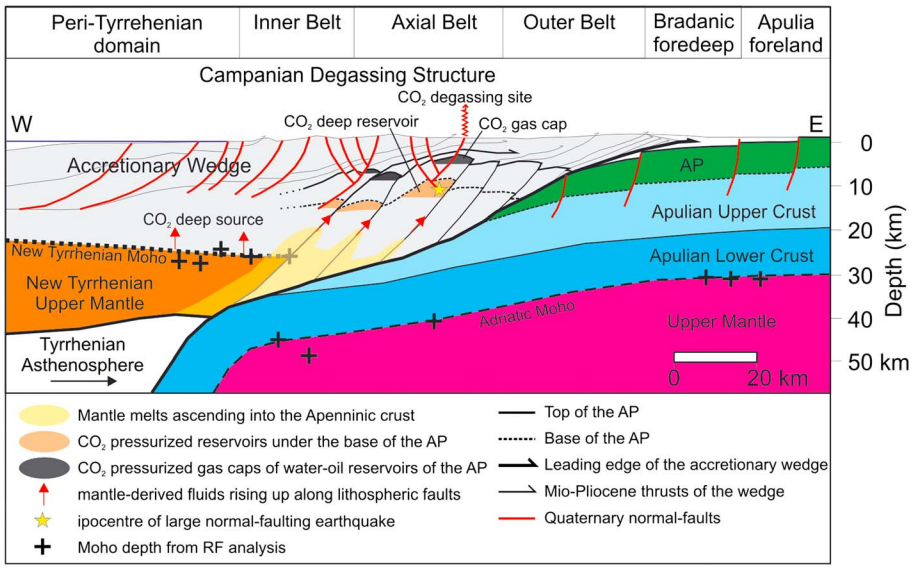

Figure 11. Cartoon summarizing our conceptual model of the degassing process of the Campanian Degassing Structure and of its relation with crustal structure, melt intrusions and seismogenesis in southern Apennines. The upwelling of the Tyrrhenian asthenospheric hot wedge that flows from the back-arc basin toward and beneath the Apennines, replacing the Adria plate, causes melting in the uppermost mantle under the belt. Melts intruded along lithospheric faults modify the thermal state of the lower and midcrust and release CO_2-rich fluids. Deep fluids migrate upward and accumulate in pressurized rock volumes under the AP and in CO_2 gas caps of the Apulian carbonate reservoirs. Active faults promote gas leakage from the caps and control locations of strong degassing sites, as Mefite d'Ansanto. The rupture process of large normal faulting earthquakes that enucleate under or at the base of the AP is influenced by high-fluid pressure in the deep CO_2 reservoirs. This model is based on the studies of *Italiano et al.* [2000], *Ghisetti and Vezzani* [2002], *Chiodini et al.* [2004], *Finetti et al.* [2005], *Frezzotti et al.* [2009], *Piana Agostinetti and Amato* [2009], and *Chiarabba and Chiodini* [2013].

7.3. Therma/Fluid Anomaly and Deep Pressurized CO_2 Reservoirs

Low-*Vp* and very low *Vp/Vs* spots suggest the existence of pressurized CO_2 rock volumes developed on top of a regional low-velocity thermal/fluid anomaly. This latter strictly correlates to low velocities in the uppermost mantle, crustal thinning, high heat flow, and intense nonvolcanic CO_2 degassing at the surface (Figure 7).

These findings yield a more comprehensive view of the Campanian Degassing Structure [*Chiodini et al.*, 2004]. The most probable source of the massive and diffuse nonvolcanic CO_2 degassing is the melting of the Tyrrhenian metasomatized mantle wedge that is rich in fluids released by the subducted Adriatic slab [*Chiodini et al.*, 2004; *Frezzotti et al.*, 2009]. Melting would be promoted by adiabatic upwelling of the hot sublithospheric mantle that flows from the Tyrrhenian back-arc basin toward and beneath the Apennines, replacing the Adriatic lithosphere (Figure 11) [*Chiarabba and Chiodini*, 2013]. In particular, *Italiano et al.* [2000] relate the Mefite d'Ansanto and other CO_2-dominated gas emissions with significant mantle-helium fluxes to mantle melts intruded into crust along lithospheric active faults. These intrusions would modify the thermal state of the lower crust-midcrust under the axial part of belt.

The regional, low-velocity anomaly we defined in the midcrust (Figures 4 and 7) fits well with the hypothesis of a thermal anomaly of *Italiano et al.* [2000]. Additionally, the idea of a link between mantle-derived fluids and active extensional faulting, introduced to explain the huge flow rate of some vents, is consistent with the model proposed here (see the cartoon shown in Figure 11). We hypothesize that deep pressurized CO_2 reservoirs (the low-*Vp/Vs* and low-*Vp* volumes) develop just below and/or within the base of the AP consisting of Triassic evaporites, where CO_2 overpressure can occur within dolostones sealed by anydrites levels [*Trippetta et al.*, 2013]. Hence, the Triassic anhydrites act as a barrier to fluid upraise and favor the formation of structural traps in which mantle-derived CO_2 can accumulates [*Chiodini et al.*, 2004]. These deep reservoirs provide a continuous recharging for the shallow, pressurized CO_2 gas caps of oil/aqueous reservoirs drilled at the top of AP in the Campanian Apennines. Fluids migrate upward along lithospheric faults connecting the deep and shallow pressurized CO_2 reservoirs. Gas leakage from the shallow caps would be promoted by

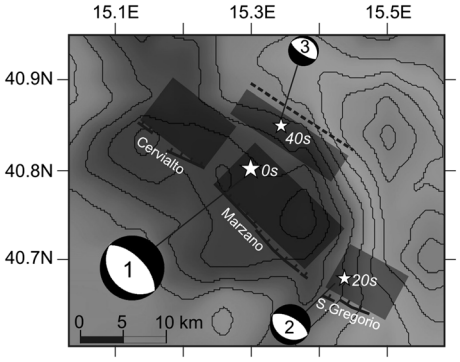

Figure 12. The fault model of the 1980 Irpinia earthquake of *Pantosti and Valensise* [1990] is superimposed on the *Vp* layer at 4 km depth. Thick black lines denote fault scarps. Numbers indicate the time progression of the rupture episodes (0 s = Marzano-Cervialto segment, 20 s = S. Gregorio segment, and 40 s = Ofanto segment). The dashed line is the surface projection of the Ofanto blind fault segment.

active normal faults that therefore control the location of the strong gas emissions, as Mefite d'Ansanto in the Mount Forcuso area.

In the Mount Forcuso area, the existence of large faults is proved by seismic commercial profiles that image deeply rooted, NW-SE trending normal faults just 2 km to the west of Mefite d'Ansanto (see documentation from ViDEPI Project, available at http://unmig.sviluppoeconomico.gov.it/deposito/videpi/relazioni/1394.pdf). The existence of large, active normal faults in the area is also supported by a few lines of evidence: (i) a strict relation between this degassing site and active faults has been recently proposed on the basis of a strong polarization of ambient seismic noise [*Pischiutta et al*., 2013], (ii) the proximity of the eastern fault segment of the 1980 Irpinia earthquake (Figure 8c), (iii) the occurrence just in the Mount Forcuso area of two destructive earthquakes in 1702 and 1732 (Figure 2), and (iv) the upraising of deep, hot fluids along Quaternary faults best explains the local, high heat flow [*Italiano et al*., 2000].

7.4. Implication on Hydrocarbon Exploration

The reconnaissance of pressurized CO_2 reservoirs under and/or within the lower sequences of the AP has a negative implication for hydrocarbon industry due to the associated risk. This problem has been already faced by companies operating in the southern Apennines after the discovery of hydrocarbon and deep-seated aqueous reservoirs with pressurized CO_2 gas caps. Gas pockets make drilling operation risky (e.g., the well Mount Forcuso 1 underwent to blowup), while hydrocarbon reservoirs strongly contaminated by CO_2 are of little interest for industry. With this study, we shed lights into the deep, magmatic origin of the CO_2 gas caps encountered in the Apulian reservoirs under the axial part of the range. Besides, we suggest that this phenomenon regards a wide portion of the Campanian arc that has not still been the target of drilling operations mainly because of the considerable depth (>5 km) of potential hydrocarbon traps.

7.5. Irpinia Fault Structure and Inference on the 1980 Earthquake

The new high-resolution model of the Irpinia region offers a retrospective vision of the 1980 *Mw*6.9 earthquake. The peculiarity of the earthquake was the multiple rupture of distinct segments delayed by tens of seconds from the first larger event [*Westaway and Jackson*, 1987; *Bernard and Zollo*, 1989; *Giardini et al*., 1996]. The source process consisted of three main rupture episodes, with nucleation times at 0, 20, and 40 s, and with $Mo = 1.6, 0.6$, and 0.4×10^{19} Nm. These shocks are thought to be generated on NW trending normal faults (Figure 12), the main, and the 20 s on NE dipping faults, the 40 s on a SW dipping antithetic plane [*Bernard and Zollo*, 1989]. Coseismic surface faulting was associated with the 0 and 20 s shocks (Figure 12), whereas the 40 s shock was ascribed to a blind fault [*Pantosti and Valensise*, 1990]. Previous tomographic models and 3-D aftershocks locations give a gross definition of the crustal structure and fault geometry and agree with aftershocks confined in the collapsing hanging wall of the NW trending conjugated faults [*Amato et al*., 1992]. *Improta et al*. [2003a] hypothesize a relation between the rupture propagation and the large-scale geometry of the AP belt defined by subsurface data and gravity modeling.

In the new velocity model, all three shocks nucleated just below the AP in the basement, with rupture that propagated upward and laterally within high-*Vp* and high-*Vp*/*Vs* regions (Figures 9b–9d). These regions mainly relate to fractured, water-saturated Apulian carbonates, as suggested by the aqueous reservoirs drilled in the AP (S. Gregorio Magno 1 well) and the low-resistivity rocks revealed by magnetotelluric data (Figure 10). Also, this interpretation is consistent with recent results of *Amoroso et al*. [2014] that defined a fault-bounded crustal block characterized by high pore pressure, water-saturated AP carbonates.

The main fault scarps associated with the 0 s shock [*Pantosti and Valensise*, 1990] developed above culminations of the AP, while the 40 s blind fault is topped by thick low-*Vp* sediments of the Ofanto satellite basin (Figure 9b). All fault segments are included in the central arc of the Apulian belt (Figure 8b) and confined to the north by the E-W lateral ramp of this arc that cuts the NNW striking structures of the Mount Forcuso Trend. So a first indication is that the segmentation is governed by lateral heterogeneity and preexisting structures of the AP, whose contractional structures rotate from NW trending to NNW trending to the north of the ruptured segments (Figure 8b).

The high-resolution Irpinia model, integrated with subsurface constraints, allows us to propose a new reconstruction of the 1980 earthquake. Seismologic and surface faulting data all showed that the 0 s shock, the main event, ruptured at least two distinct segments of the main seismogenic structure striking NW-SW and dipping 60° toward the NE (Marzano and Cervialto sections, in Figure 12). *Bernard and Zollo* [1989]; *Cocco and Pacor* [1993] and *Giardini et al*. [1996] indicate that rupture propagated both south-westward and north-westward for a total length of about 30 km and a duration of 12–13 s. Summing up the coseismic fault scarps recognized by *Pantosti and Valensise* [1990] we arrive to a similar extent of 32 km. So given the uncertainties in the hypocenter of the 0 s shock [see *Giardini et al*., 1996] and in the fault length defined by surface ruptures or modeling of seismological and geodetic data, we hypothesize that the 0 s shock broke entirely from the Cervialto segment in the north to the S. Gregorio segment in the south (Figure 12). In this new model, the 32 km long surface ruptures are entirely associated with the 0 s shock. The deepening of the high-*Vp* AP south-westward of the 0 s section (Figure 9d) can account for the complex pattern of surface scarps recognized in the S. Gregorio area by *Pantosti and Valensise* [1990]. Also, this reconstruction fits better paleoseismology data that reveal a concomitant rupture of the Marzano and S. Gregorio segments during at least five paleoevents [*Pantosti et al*., 1993]. In addition, we remark that the geologic seismic moment estimated by *Pantosti and Valensise* [1990] for the Cervialto, Marzano, and S. Gregorio segments equals the seismic moment (e.g., 1.6×10^{19} Nm) estimated for the 0 s shock from long-period recordings by *Giardini et al*. [1996].

We propose that both the 20 s and the 40 s subevents originated on antithetic faults, reactivating West dipping thrust faults at the eastern edge of the Apulian belt. In the tomographic model there are strong indications for a high-angle thrust nearby the hypocenter of the 40 s shock. Specifically, the abrupt eastward deepening of the high-velocity AP accompanied to a West dipping low-velocity zone (Figure 9b). Additionally, that fault perfectly matches the buried ramp of the central arc of the Apulian belt (Figure 8b). We extend the antithetic fault hypothesis to the 20 s subevent that was until now ascribed to a NE dipping low-angle normal fault [*Bernard and Zollo*, 1989; *Pingue et al*., 1993]. Again, a West dipping thrust fault referable to the Vallauria Trend is well documented close to the hypocenter by our tomography (Figure 9c) and by subsurface data (Figure 8b).

Differently from the two antithetic segments, there is no indication for the fault ruptured during the 0 s shock in the section shown in Figure 9b. We note that this is not in contradiction with previous conclusions because it is well established that the 0 s shock ruptured a late Pleistocene fault with a small cumulative vertical displacement, in the order of 30–40 m [*Improta et al*., 2003b; *Bruno et al*., 2010].

We remind that the previous interpretation of the 20 s subevent opens several problems. There is no evidence both in the field and in the crustal images from seismic exploration and tomography that an E dipping low-angle normal fault exists in the area. Since the extensional regime is young, such a fault cannot derive from rotation of high-angle faults and reasonably is a reactivation of an existing thrust. Again, there is no indication for the presence of an E dipping low-angle thrust (e.g., back-thrust) in the upper crust [*Scrocca et al*., 2005]. Similar evidences for thrust reactivation by normal faulting earthquakes are striking for the 2009 L'Aquila sequence in central Apennines [*Chiarabba et al*., 2009; *Valoroso et al*., 2013]. Additionally, this new model overcomes the decennial discussion on the inconsistency of the sources of the 20 s shock based on geodetic (e.g., low-angle) [*Pingue et al*., 1993] or surface faulting data (e.g., high-angle) [*Pantosti and Valensise*, 1990], and it is not in contrast with leveling line data that show an almost symmetric subsidence across the 20 s fault [*Pingue et al*., 1993] and do not allow to constrain unambiguously the fault dip [see *Amoruso et al*., 2005]. We recognize that the low-angle plane of the 20 s event focal mechanism is the E dipping [*Bernard and Zollo*, 1989], but the uncertainties on the dip angle of the solution, not even reported, are presumably not small.

With respect to previous [*Amato et al*., 1992] and recently published [*Amoroso et al*., 2014] models of the Irpinia fault area, our study provides evidence of a deep low-*Vp*/*Vs* region beneath the AP at the depth of nucleation of the 1980 main shock. This result allows us to propose a new interpretation of the rupture process for this complex earthquake. The rupture of the first shock started inside the low-*Vp*/*Vs* volume and propagated preferentially upward inside the high-*Vp* and high-*Vp*/*Vs* regions (Figures 9b and 9d). We hypothesize that high-fluid pressure in the deep CO_2 reservoir (the low-*Vp*/*Vs* volume) played a key role in the rupture that enucleated just under the AP. This hypothesis is in agreement with the recent study of *Ciotoli et al*. [2014] that relates soil gas anomalies along the 1980 surface ruptures to deep-seated gas (including deep origin CO_2) migrating along the fault segments. Then, the main shock rupture propagated preferentially within high-*Vp* main asperities located inside the Apulian carbonates. A link between broken asperities and Apulian carbonates is suggested by the good correspondence found between the regions of highest-slip velocity [*Cocco and Pacor*, 1993] and the very high velocity spot (*Vp* = 6.2–6.6 km/s) defined along the 0 s fault segment at 4–6 km under the Marzano ridge (Figure 9b). Also, very high *Vp*/*Vs* Apulian carbonates crossed by the 0 s fault segment (Figures 9b and 9d) indicate that high pore pressure in water-saturated carbonates controlled the rupture process, as recently proposed by *Amoroso et al*. [2014].

As the high-velocity region along the fault terminates, the 0 s rupture stopped and the conjugate faults were activated. Figure 8b outlines an intriguingly coincidence among the northern and southern ends of the main seismogenic structure ruptured during the 0 s shock, low-*Vp* zones, and the lateral ramps of the central arc of the Apulian belt. One explanation could be that rupture stopped entering the low-*Vp* regions that follow the thrust faults. The former could correspond to strongly fractured low-strength zones with stable sliding behavior. Alternatively, low-*Vp* regions could evidence lithological heterogeneities across thrust faults. Conversely, very high velocities in the AP are indicative of high-strength carbonates characterized by unstable sliding. Very high velocity, high-strength rocks likely correspond to Triassic-Jurassic dolostones, eventually intruded by Paleogene gabbroic dikes, as those drilled by the well S. Gregorio Magno 1 (Figure 10a).

At a larger scale, we note that recent seismicity under the axial zone of the belt concentrates in the upper 12–14 km of the crust [*Di Stefano et al*., 2009], inside the Apulian carbonates and the underlying basement, and mostly follows the culminations of the Inner AP (Figure 2). Also, the occurrence of large historical earthquakes appears correlated to wide antiforms of the AP (Figure 2). This overall correspondence between the geometry of the extensional seismic belt and of the Apulian belt suggests that inherited structures, developed during Pliocene-early Pleistocene compression, control the seismicity and the segmentation of the seismogenic fault system, as observed for the 1980 Irpinia earthquake. The role played by inherited structures of the thrust-fold-belt on the geometry and kinematics of active faults has been widely documented in southern Apennines [*Vitale et al*., 2012]. In a recent paper, *Ascione et al*. [2013] analyze morphotectonic and subsurface data concluding that the structures capable of nucleating large earthquakes in the Irpinia region are inherited basement faults reactivated in the current extensional tectonic regime. The correspondence found in our study among the 20 s and 40 s faults segments of the 1980 earthquake and thrust faults unraveled by the comparison of high-resolution *Vp* images with subsurface data [*Nicolai and Gambini*, 2007] reinforces previous interpretations that preexisting structures of the Apulian belt controlled the rupture propagation [*Amato et al*., 1992; *Improta et al*., 2003a; *Ascione et al*., 2013].

All the larger ($M_L > 4$) earthquakes occurred along the axial zone of the belt since 1984 are located above the low-*Vp* thermal/fluid anomaly (Figure 7). The identification of pressurized CO_2 reservoirs on top of this anomaly, at about the hypocentral depth of the large normal faulting earthquakes of southern Apennines (e.g., 10–12 km depth), points to a role of high-pressure fluids in the seismogenesis. A relation between seismicity and high-fluid pressure at depth was already proposed for the central Apennines based on the coincidence between crustal seismicity and CO_2 degassing areas [*Ghisetti and Vezzani*, 2002; *Chiodini et al*., 2004; *Chiarabba and Chiodini*, 2013]. The role played by pressure diffusions from deep, pressurized CO_2 volumes in triggering earthquakes is striking for the 1997 Colfiorito sequence [*Miller et al*., 2004]. Our previous considerations on the nucleation of the 0 s shock of the Irpinia earthquake support and extend this idea to the whole Apennines. We propose a suggestive scenario in which CO_2-rich fluids of mantle origin are stocked in pressurized reservoirs developed just under the AP and/or inside its Triassic

lower sequence, where periodic overpressure leads to the triggering of large normal faulting earthquakes. Hence, the rupture process of large normal faulting events is conditioned by the presence of Triassic anhydrites at the base of the AP, which favors the formation of structural traps in which mantle-derived CO_2 can accumulate (see the cartoon in Figure 11).

8. Conclusions

The main result of our study is the identification under the external Apennines of high-*Vp*, high-susceptibility, low-resistivity bodies in the upper crust/midcrust of the Apulian plate. These bodies are interpreted as large mafic intrusions and related to the anorogenic intraplate magmatism developed in the Adriatic domain during Paleogene. This interpretation is supported by the reconnaissance in numerous wells of Paleocene-Eocene mafic intrusions and thick basalt extrusions, with the latter coeval with crustal extension and drowning of AP [*Cippitelli*, 2007]. These findings have two wide implications. First, the Paleogene magmatism that until now was documented in southern Italy only by the small intrusion of Pietre Nere [*Bigazzi et al*., 1996] affected a broad portion of the Apulian crust actually buried under the external Apennines. Second, it supports the model of *Lustrino and Wilson* [2007] that relates the Paleogene magmatism to passive upwelling and adiabatic decompression of the astenospheric mantle in response to lithosphere extension. The Outer AP was also affected by a minor, prior to this study substantially unknown, episode of basic volcanism presumably during upper Miocene. Although the origin of this episode is unclear, this coincidence suggests the occurrence of a weakness zone in the stretched Apulian lithosphere that drove the ascent of mantle melts and the formation of large intrusions into the crust under the external Apennines. Intriguingly, the Pleistocene volcanism of Mount Vulture took place just above the presumed weakness zone. This reconciles with the strong intraplate signature of Mount Vulture, ascribed to an asthenospheric source beneath the Adriatic plate [*De Astis et al*., 2006].

Our conclusions should spur detailed petrological analysis of the Cenozoic mafic rocks that were cored in numerous wells (see Table S2). Until now, petrological data were limited to the Pietre Nere [*Bigazzi et al*., 1996; *De Astis et al*., 2006], whereas new data from cores could led to a comprehensive view of the Cenozoic magmatism of the Apulian domain.

The new tomographic models cannot definitely resolve the ambiguity regarding the deep structure and Pliocene evolution of southern Apennines. Rather, we suggest that previous interpretations of high-velocity or high-susceptibility bodies in terms of crystalline basement thrusts incorporated in the belt should be reconsidered [*Speranza and Chiappini*, 2002; *Improta and Corciulo*, 2006]. Anyway, the deep part of the Irpinia model, integrated with RF constraints [*Steckler et al*., 2008], seems to be more consistent with a thick-skinned structure of the Pliocene Apulian belt.

Our investigation reinforces with independent observations geochemical models of CO_2 degassing and high heat flow originated by mantle melts intruded into the axial part of the belt [*Italiano et al*., 2000; *Chiodini et al*., 2004; *Chiarabba and Chiodini*, 2013]. The midcrustal, low-velocity thermal/fluids anomaly defined under the western part of the mountain belt is coherent with previous geochemical models. Additionally, the identification of gas-pressurized rock volumes developed under the AP has wide implications not only for a better understanding of surface gas emissions and CO_2 gas caps in the Apulian reservoirs but also for the relationship among deep fluids, active faults, and seismogenesis.

By combining the fine-scale Irpinia model with hydrocarbon exploration data, we propose a new reconstruction of the 1980 *Mw*6.9 earthquake. The 0 s shock nucleated under the AP in the basement, likely at the top of a pressurized CO_2 reservoir. This is the first indication that high-pressure CO_2 of deep origin played a role in the nucleation of the rupture, similarly to what observed for the 1997 Colfiorito and the 2009 L'Aquila sequences in central Apennines [*Miller et al*., 2004; *Lucente et al*., 2010]. Rupture propagation was controlled by the extent of high-velocity high-strength regions in the AP and by lithological-rheological heterogeneity along preexisting thrust faults. We ascribe the 0 s shock to a main seismogenic structure that extends from the Cervialto segment in the north to the S. Gregorio segment in the south, and both subevents to antithetic structures reactivating thrust faults of the Apulian belt. This model, in which the entire fault scarp is ascribed to the 0 s main rupture, overcomes the decennial discussion on the geologic versus geodetic source of the 20 s shock.

Acknowledgments

P- and *S*-arrival times of local earthquakes recorded by the ISNet network used in this study were provided in the framework of the S5 Project "High-resolution multidisciplinary monitoring of active fault test-site areas in Italy; Test site Irpinia Fault System" (Task 3, responsible A. Zollo, University of Naples). The S5 Project was financially supported by the Italian Civil Protection Department (DPC Projects 2007–2009). Arrival times data are available at http://dpc-s5.rm.ingv.it/it/ScientificReport.html. Etta Patacca and the Associate Editor are gratefully acknowledged for their comments. We thank Guido Ventura and Gianfilippo De Astis for fruitful discussions.

References

Amato, A., C. Chiarabba, L. Malagnini, and G. Selvaggi (1992), Three dimensional P-velocity structure in the region of normal faulting, the Ms = 6.9 Irpinia, Italy, earthquake, *Phys. Earth. Planet. Int.*, *75*, 111–119, doi:10.1016/0031-9201(92)90122-C.

Amoroso, O., A. Ascione, S. Mazzoli, J. Virieux, and A. Zollo (2014), Seismic imaging of a fluid storage in the actively extending Apennine mountain belt, southern Italy, *Geophys. Res. Lett.*, *41*, 3802–3809, doi:10.1002/2014GL060070.

Amoruso, A., L. Crescentini, and R. Scarpa (2005), Faulting geometry for the complex 1980 Campania-Lucania earthquake from levelling data, *Geophys. J. Int.*, *162*, 156–168, doi:10.1111/j.1365-246X.2005.02652.x.

Anelli, L., V. Cappelli, E. Cassano, I. Giori, and P. La Torre (2007), Integrated interpretation of the magnetic and gravity data along the seismic line CROP-04, in *Results of the CROP Project, Sub-Project CROP-04 Southern Apennines (Italy)*, edited by A. Mazzotti, E. Patacca, and P. Scandone, Ital. J. Geosci., vol. 7, pp. 257–266, Bollettino della Societa Geologica, Italiana, Rome.

Ascione, A., S. Mazzoli, P. Petrosino, and E. Valente (2013), A decoupled kinematic model for active normal faults: Insights from the 1980, Ms = 6.9 Irpinia earthquake, southern Italy, *Geol. Soc. Am. Bull.*, *125*, 1239–1259, doi:10.1130/B30814.1.

Avanzinelli, R., M. Lustrino, M. Mattei, L. Melluso, and S. Conticelli (2009), Potassic and ultrapotassic magmatism in the circum-Tyrrhenian region: Significance of carbonated pelitic vs. pelitic sediment recycling at destructive plate margins, *Lithos*, *113*(1–2), 213–227, doi:10.1016/j.lithos.2009.03.029.

Beccaluva, L., M. Coltorti, P. Di Girolamo, L. Melluso, L. Milani, V. Morra, and F. Siena (2002), Petrogenesis and evolution of Mt.Vulture alkaline volcanism (southern Italy), *Mineral. Petrol.*, *74*, 277–297, doi:10.1007/s007100200007.

Bernard, P., and A. Zollo (1989), The Irpinia (Italy) 1990 earthquake: Detailed analysis of a complex normal fault, *J. Geophys. Res.*, *94*, 1631–1648, doi:10.1029/JB094iB02p01631.

Bianchini, G., L. Beccaluva, and F. Siena (2008), Post-collisional and intraplate Cenozoic volcanism in the rifted Apennines/Adriatic domain, *Lithos*, *101*, 125–140, doi:10.1016/j.lithos.2007.07.011.

Bigazzi, G., M. A. Laurenzi, C. Principe, and D. Brocchini (1996), New geochronological data on Igneous rocks and evaporites of the Pietre Nere point (Gargano peninsula, southern Italy), *Boll. Soc. Geol. Ital.*, *115*, 439–448.

Bigi, S., and P. Costa Pisani (2005), From a deformed Peri-Tethyan carbonate platform to a fold-and-thrust belt: An example from the Central Apennines (Italy), *J. Struct. Geol.*, *27*, 523–539, doi:10.1016/j.jsg.2004.10.005.

Bisio, L., R. Di Giovanbattista, G. Milano, and C. Chiarabba (2004), Three-dimensional earthquake locations and upper crustal structure of the Sannio-Matese region (southern Italy), *Tectonophysics*, *385*, 121–136, doi:10.1016/j.tecto.2004.01.007.

Bruno, P. P., A. Castiello, and L. Improta (2010), Ultrashallow seismic imaging of the causative fault of the 1980, M6.9, southern Italy earthquake by pre-stack depth migration of dense wide-aperture data, *Geophys. Res. Lett.*, *37*, L19302, doi:10.1029/2010GL044721.

Butler, R. W. H., et al. (2004), Applying thick-skinned tectonic model to the Apennine thrust-belt of Italy: Limitations and implications, in *Thrust Tectonic and Hydrocarbon System*, edited by K. R. McClay, *Mem. AAPG*, 82, 647–667.

Caratori Tontini, F., P. Stefanelli, I. Giori, O. Faggioni, and C. Carmisciano (2004), The revised aeromagnetic anomaly map of Italy, *Ann. Geofis.*, *47*(5), 1547–1556.

Casero, P., F. Roure, and R. Vially (1991), Tectonic framework and petroleum potential of the southern Apennines, in *Generation, Accumulation, and Production of Europe's Hydrocarbons*, Spec. Publ., vol. 1, edited by A. M. Spencer, pp. 381–387, European Association of Petroleum Geoscientists, Berlin.

Chatelain, J. L. (1978), Etude fine de la sismicité en zone de collision continentale aumoyen d'un réseau de stations portables: La région Hindu-Kush Pamir. Thèse de doctorat de 3ème cycle Université scientifique et médicale de Grenoble, 219 pp.

Chiarabba, C., and A. Amato (1997), Upper-crustal structure of the Benevento area (southern Italy): Fault heterogeneities and potential for large earthquakes, *Geophys. J. Int.*, *130*, 229–239, doi:10.1111/j.1365-246X.1997.tb01001.x.

Chiarabba, C., and G. Chiodini (2013), Continental delamination and mantle dynamics drive topography, extension and fluid discharge in the Apennines, *Geology*, *41*(6), 715–718, doi:10.1130/G33992.1.

Chiarabba, C., L. Jovane, and R. Di Stefano (2005), A new view of Italian seismicity using 20 years of instrumental recordings, *Tectonophysics*, *395*, 251–268, doi:10.1016/j.tecto.2004.09.013.

Chiarabba, C., P. De Gori, and E. Boschi (2009), Pore-pressure migration along a normal-fault system resolved by time-repeated seismic tomography, *Geology*, *37-1*, 67–70, doi:10.1130/G25220A.1.

Chiodini, G., C. Cardellini, A. Amato, E. Boschi, S. Caliro, F. Frondini, and G. Ventura (2004), Carbon dioxide Earth degassing and seismogenesis in central and southern Italy, *Geophys. Res. Lett.*, *31*, L07615, doi:10.1029/2004GL019480.

Chiodini, G., D. Granieri, R. Avino, S. Caliro, A. Costa, C. Minopoli, and G. Vilardo (2010), Non-volcanic CO2 Earth degassing: Case of Mefite d'Ansanto (southern Apennines), Italy, *Geophys. Res. Lett.*, *37*, L11303, doi:10.1029/2010GL042858.

Cinque, A., E. Patacca, P. Scandone, and M. Tozzi (1993), Quaternary kinematic evolution of the southern Apennines, *Ann. Geophys.*, *36*(2), 249–260.

Ciotoli, G., S. Bigi, C. Tartarello, P. Sacco, S. Lombardi, A. Ascione, and S. Mazzoli (2014), Soil gas distribution in the main coseismic surface rupture zone of the 1980, Ms = 6.9, Irpinia earthquake (southern Italy), *J. Geophys. Res. Solid Earth*, *119*, 2440–2461, doi:10.1002/2013JB010508.

Cippitelli, G. (2007), The CROP-04 seismic profile: Interpretation and structural setting of the Agropoli-Barletta Geotraverse, in *Results of the CROP Project, Sub-Project CROP-04 Southern Apennines (Italy)*, Ital. J. Geosci., vol. 7, edited by A. Mazzotti, E. Patacca, and P. Scandone, pp. 267–281, Bollettino della Società Geologica Italiana, Rome.

Cocco, M., and F. Pacor (1993), The rupture process of the 1980, Irpinia, Italy earthquake from the inversion of strong motion waveforms, *Tectonophysics*, *218*, 157–177.

CPTI Working Group (2004), Catalogo Parametrico dei Terremoti Italiani, v. 2004 (CPTI04), INGV, Bologna. [Available at http://emidius.mi.ingv.it/CPTI04/.]

D'Agostino, N., A. Avallone, D. Cheloni, E. D'Anastasio, S. Mantenuto, and G. Selvaggi (2008), Active tectonics of the Adriatic region from GPS and earthquake slip vectors, *J. Geophys. Res.*, *113*, B12413, doi:10.1029/2008JB005860.

De Astis, G., P. D. Kempton, A. Peccerillo, and T. W. Wu (2006), Trace element and isotopic variations from Mt. Vulture to Campanian volcanoes: Constraints for slab detachment and mantle inflow beneath southern Italy, *Contrib. Mineral. Petrol.*, *151*, 331–351, doi:10.1007/s00410-006-0062-y.

Della Vedova, B., S. Bellani, G. Pellis, and P. Squarci (2001), Deep temperatures and surface heat flow distribution, in *Anatomy of a Mountain: The Apennines and Adjacent Mediterranean Basins*, edited by G. B. Vai and I. P. Martini, pp. 65–76, Kluwer Acad., Dordrecht, Netherlands.

Dewey, J. F., M. L. Helman, E. Turco, D. W. H. Hutton, and S. P. Knott (1989), Kinematics of the western Mediterranean, in *Alpine Tectonics*, edited by M. P. Coward, D. Dietrich, and R. G. Park, *Geol. Soc. London Spec. Publ.*, *45*, 265–283.

Di Stefano, R., E. Kissling, C. Chiarabba, A. Amato, and D. Giardini (2009), Shallow subduction beneath Italy: Three-dimensional images of the Adriatic-European-Tyrrhenian lithosphere system based on high-quality P wave arrival times, *J. Geophys. Res.*, *114*, B05305, doi:10.1029/2008JB005641.

Doglioni, C., P. Harabaglia, G. Martinelli, F. Mongelli, and G. Zito (1996), A geodynamic model of the southern Apennines accretionary prism, *Terra Nova*, *8*, 540–547.

Eberhart-Phillips, D. (1993), Local earthquake tomography: Earthquake source regions, in *Seismic Tomography: Theory and Practice*, edited by H. M. Iyer and K. Hirahara, pp. 613–643, Chapman and Hall, London, U. K.

Eberhart-Phillips, D., and N. Chadwick (2002), Three-dimensional attenuation model of the shallow Hikurangi subduction zone in the Raukumura Peninsula, New Zealand, *J. Geophys. Res.*, *107*(B2), 2033, doi:10.1029/2000JB000046.

Eberhart-Phillips, D., and M. Reyners (1997), Continental subduction and three-dimensional crustal structure: The Northern South Island, New Zeland, *J. Geophys. Res.*, *102*, 11,843–11,861, doi:10.1029/96JB03555.

Faccenna, C., T. Becker, F. Lucente, L. Jolivet, and F. Rossetti (2001), History of subduction and back-arc extension in the central Mediterranean, *Geophys. J. Int.*, *145*, 809–820, doi:10.1046/j.0956-540x.2001.01435.x.

Finetti, I. R., F. Lentini, S. Carbone, A. Del Ben, A. Di Stefano, P. Guarnieri, M. Pipan, and A. Prizzon (2005), Crustal tectono-stratigraphy and geodynamics of the southern Apennines from crop and other integrated geophysical-geological data, in *CROP Project 1: Deep Seismic Exploration of the Central Mediterranean and Italy*, edited by I. R. Finetti, pp. 225–262, Elsevier, Amsterdam.

Frezzotti, M. L., A. Peccerillo, and G. Panza (2009), Carbonate metasomatism and CO_2 lithosphere-asthenosphere degassing beneath the Western Mediterranean: An integrated model arising from petrological and geophysical data, *Chem. Geol.*, *262*, 108–120, doi:10.1016/j.chemgeo.2009.02.015.

Ghisetti, F., and L. Vezzani (2002), Normal faulting, transcrustal permeability and seismogenesis in the Apennines (Italy), *Tectonophysics*, *348*, 155–168.

Giacomuzzi, G., C. Chiarabba, and P. De Gori (2011), Linking the Alps and Apennines subduction systems: New constraints revealed by high-resolution teleseismic tomography, *Earth Planet. Sci. Lett.*, *301*(3–4), 531–543, doi:10.1016/j.epsl.2012.05.004.

Giacomuzzi, G., M. Civalleri, P. De Gori, and C. Chiarabba (2012), A 3D Vs model of the upper mantle beneath Italy: Insight on the geodynamics of central Mediterranean, *Earth Planet. Sci. Lett.*, *335–336*, 105–120, doi:10.1016/j.epsl.2010.11.033.

Giardini, D., A. Basili, and E. Boschi (1996), Applying the relative hypocentre location approach: Where was the 1980 November 23 Irpinia earthquake?, *Geophys. J. Int.*, *127*(3), 605–615, doi:10.1111/j.1365-246X.1996.tb04041.x.

Haslinger, F. (1998), Velocity structure, seismicity and seismotectonics of northwestern Greece between the Gulf of Arta and Zakynthos, PhD thesis, Dep. Geophys., ETH, Zurich, Switzerland.

Iannaccone, G., et al. (2010), A prototype system for earthquake early-warning and alert management in southern Italy, *Bull. Earthquake Eng.*, *2010*(8), 1105–1129, doi:10.1007/s10518-009-9131-8.

Improta, L., and M. Corciulo (2006), Controlled source non-linear tomography: A powerful tool to constrain tectonic models of the southern Apennines orogenic wedge, Italy, *Geology*, *34*(11), 941–944, doi:10.1130/G22676A.1.

Improta, L., G. Iannaccone, P. Capuano, A. Zollo, and P. Scandone (2000), Inferences on upper crustal structure of the southern Apennines (Italy) from seismic refraction investigations and subsurface data, *Tectonophysics*, *317*, 275–298, doi:10.1016/S0040-1951(99)00267-X.

Improta, L., M. Bonagura, P. Capuano, and G. Iannaccone (2003a), An integrated geophysical investigation of the upper crust in the epicentral area of the 1980, Ms6.9, Irpinia earthquake (southern Italy), *Tectonophysics*, *361*(1–2), 139–169, doi:10.1016/S0040-1951(02)00588-7.

Improta, L., A. Zollo, P. P. Bruno, A. Herrero, and F. Villani (2003b), High resolution seismic tomography across the 1980 (Ms 6.9) southern Italy earthquake fault scarp, *Geophys. Res. Lett.*, *30*(10), 1494, doi:10.1029/2003GL017077.

Italiano, F., M. Martelli, G. Martinelli, and P. M. Nuccio (2000), Geochemical evidence of melt intrusions along lithospheric faults of the southern Apennines, Italy: Geodynamic and seismogenic implications, *J. Geophys. Res.*, *105*(B6), 13,569–13,578, doi:10.1029/2000JB900047.

Lahr, J. C. (1989), HYPOELLIPSE/VERSION 2.0: A computer program for determining local earthquake hypocentral parameters, magnitude and first motion pattern. *U.S. Geol. Surv. Open File Rep.*, *89-116*, 92 pp.

Loddo, M., R. Quarto, and D. Schiavone (1996), Integrated geophysical survey for the geological structural and hydrogeothermal study of the North-western Gargano promontory (southern Italy), *Ann. Geofis.*, *39*(1), 201–219.

Lucente, F. P., L. Margheriti, C. Piromallo, and G. Barruol (2006), Seismic anisotropy reveals the long route of the slab through the western-central Mediterranean mantle, *Earth Planet. Sci. Lett.*, *241*(3–4), 517–529.

Lucente, F. P., P. De Gori, L. Margheriti, D. Piccinini, M. Di Bona, C. Chiarabba, and N. P. Agostinetti (2010), Temporal variation of seismic velocity and anisotropy before the 2009 Mw 6.3 L'Aquila earthquake, Italy, *Geology*, *38*, 1015–1018, doi:10.1130/G31463.1.

Lustrino, M., and M. Wilson (2007), The circum-Mediterranean anorogenic Cenozoic igneous province, *Earth Sci. Rev.*, *81*, 1–65, doi:10.1016/j.earscirev.2006.09.002.

Macera, P., D. Gasperini, C. Piromallo, J. Blichert-Toft, D. Bosch, A. Del Moro, and S. Martin (2003), Geodynamic implications of deep mantle upwelling in the source of Tertiary volcanics from the Veneto region (South-Eastern Alps), *J. Geodyn.*, *36*, 563–590.

Mackenzie, G. D., H. Thybo, and P. K. H. Maguire (2005), Crustal velocity structure across the Main Ethiopian Rift: Results from two-dimensional wide-angle seismic modelling, *Geophys. J. Int.*, *162*(3), 994–1006, doi:10.1111/j.1365-246X.2005.02710.x.

Maggi, C., A. Frepoli, G. B. Cimini, R. Console, and M. Chiappini (2009), Recent seismicity and crustal stress field in the Lucanian Apennines and surrounding areas (southern Italy): Seismotectonic implications, *Tectonophysics*, *463*(1–4), 130–144, doi:10.1016/j.tecto.2008.09.032.

Malinverno, A., and W. B. F. Ryan (1986), Extension in the Tyrrhenian Sea and shortening in the Apennines as a result of arc migration driven by sinking of the lithosphere, *Tectonics*, *5*, 227–245, doi:10.1029/TC005i002p00227.

Marzocchi, W., A. Amato, A. Akinci, C. Chiarabba, A. M. Lombardi, D. Pantosti, and E. Boschi (2012), A ten-year earthquake occurrence model for Italy, *Bull. Seismol. Soc. Am.*, *102*(3), 1195–1213, doi:10.1785/0120110164.

Matrullo, E., R. De Matteis, C. Satriano, O. Amoroso, and A. Zollo (2013), An improved 1-D seismic velocity model for seismological studies in the Campania-Lucania region (southern Italy), *Geophys. J. Int.*, *195*, 460–473, doi:10.1093/gji/ggt224.

Mazzoli, S., S. Barkham, G. Cello, R. Gambini, L. Mattioni, P. Shiner, and E. Tondi (2001), Reconstruction of continental margin architecture deformed by the contraction of the Lagonegro Basin, southern Apennines, Italy, *J. Geol. Soc. London*, *158*, 309–319, ISSN: 0016-7649.

Mazzoli, S., M. D'Errico, L. Aldega, S. Corrado, C. Invernizzi, P. Shiner, and M. Zattin (2008), Tectonic burial and 'young' (<10 Ma) exhumation in the southern Apennines fold and thrust belt (Italy), *Geology*, *36*, 243–246, doi:10.1130/G24344A.1.

Mazzotti, A. P., E. Stucchi, G. L. Fradelizio, L. Zanzi, and P. Scandone (2000), Seismic exploration in complex terrains: A processing experience in the southern Apennines, *Geophysics*, *65*(5), 1402–1417, doi:10.1190/1.1444830.

Menardi Noguera, A., and G. Rea (2000), Deep structure of the Campania-Lucanian arc (southern Apennine, Italy), *Tectonophysics*, *324*, 239–265.

Michelini, A., and T. V. McEvilly (1991), Seismological studies at Parkfield. I. Simultaneous inversion for velocity structure and hypocenters using cubic B-splines parameterization, *Bull. Seismol. Soc. Am.*, *81*, 524–552.

Miller, S. A., C. Collettini, L. Chiaraluce, M. Cocco, M. Barchi, and B. J. P. Kaus (2004), Aftershocks driven by a high-pressure CO_2 at depth, *Nature*, *427*, 724–727, doi:10.1038/nature02251.

Mongelli, F., P. Harabaglia, G. Martinelli, P. Squarci, and G. Zito (1996), Nuove misure di flusso geotermico in Italia meridionale: Possibili implicazioni sismotettoniche, in *Atti del 14° Convegno del Gruppo Naz. di Geofisica della Terra Solida*, pp. 929–939, Consiglio Nazionale delle Ricerche, Rome.

Moretti, M., P. Pieri, G. Ricchetti, and L. Spalluto (2011), Note Illustrative della Carta Geologica d'Italia alla scala 1:50.000, F°396 San Severo. ISPRA and Servizio Geologico di Stato, Rome.

Mostardini, F., and S. Merlini (1986), Appennino centro-meridionale. Sezioni geologiche e proposta di modello strutturale, *Mem. Soc. Geol. Ital.*, *35*, 177–202.

Nicolai, C., and R. Gambini (2007), Structural architecture of the Adria platform-and-basin system, in *Results of the CROP Project, Sub-Project CROP-04 Southern Apennines (Italy)*, Ital. J. Geosci., vol. 7, edited by A. Mazzotti, E. Patacca, and P. Scandone, pp. 21–37, Bollettino della Società Geologica Italiana, Rome.

Pantosti, D., and G. Valensise (1990), Faulting mechanism and complexity of the November 23, 1980, Campania-Lucania earthquake, inferred from surface observations, *J. Geophys. Res.*, *95*(15), 319–341, doi:10.1029/JB095iB10p15319.

Pantosti, D., D. P. Schwartz, and G. Valensise (1993), Paleoseismolgy along the 1980 surface rupture of the Irpinia fault: Implications for earthquake recurrence in the southern Apennines, Italy, *J. Geophys. Res.*, *98*(B4), 6561–657, doi:10.1029/92JB02277.

Patacca, E. (2007), Stratigraphic constraints on the CROP-04 seismic line interpretation: San Fele 1, Monte Foi 1, and San Gregorio Magno 1 wells (southern Apennines, Italy), in *Results of the CROP Project, Sub-Project CROP-04 Southern Apennines (Italy)*, Ital. J. Geosci., vol. 7, edited by A. Mazzotti, E. Patacca, and P. Scandone, pp. 185–239, Bollettino della Società Geologica Italiana, Rome.

Patacca, E., and P. Scandone (1989), Post-Tortonian mountain building in the Apennines. The role of the passive sinking of a relic lithospheric slab, in *The Lithosphere in Italy: Advances in Earth Science Research*, vol. 80, edited by A. Boriani et al., pp. 157–176, Accademia Nazionale dei Lincei, Rome.

Patacca, E., and P. Scandone (2001), Late thrust propagation and sedimentary response in the thrust belt-foredeep system of the southern Apennines (Pliocene-Pleistocene), in *Anatomy of a Mountain: The Apennines and Adjacent Mediterranean Basins*, edited by G. B. Vai and I. P. Martini, pp. 401–440, Kluwer Acad., Dordrecht, Netherlands.

Patacca, E., and P. Scandone (2007), Geological interpretation of the CROP-04 seismic line (southern Apennines, Italy), in *Results of the CROP Project, Sub-Project CROP-04 Southern Apennines (Italy)*, Ital. J. Geosci., vol. 7, edited by A. Mazzotti, E. Patacca, and P. Scandone, pp. 297–315, Bollettino della Società Geologica Italiana, Rome.

Patacca, E., R. Sartori, and P. Scandone (1990), Tyrrhenian basin and Apenninic arcs: Kinematic relations since Late Tortonian times, *Mem. Soc. Geol. Ital.*, *45*, 425–451.

Patella, D., Z. Petrillo, A. Siniscalchi, L. Improta, and B. Di Fiore (2005), Magnetotelluric profiling along the crop-04 section in the southern Apennines, in *CROP Project 1, Deep Seismic Exploration of the Central-Mediterranean and Italy*, edited by I. R. Finetti, Elsevier, Amsterdam.

Pavlis, G. L., and J. R. Booker (1980), The mixed discrete-continuous inverse problem: Application to the simultaneous determination of earthquake hypocenters and velocity structure, *J. Geophys. Res.*, *85*, 4801–4810, doi:10.1029/JB085iB09p04801.

Peccerillo, A. (1999), Multiple mantle metasomatism in central-southern Italy: Geochemical effects, timing and geodynamic implications, *Geology*, *27*, 315–318, doi:10.1130/0091-7613(1999)027<0315:MMMICS>2.3.CO;2.

Piana Agostinetti, N., and A. Amato (2009), Moho depth and *Vp/Vs* ratio in peninsular Italy from teleseismic receiver function, *J. Geophys. Res.*, *114*, B06303, doi:10.1029/2008JB005899.

Pingue, F., G. De Natale, and P. Briole (1993), Modeling of the 1980 Irpinia source: Constraints from geodetic data, *Ann. Geofis.*, *34*(1), 27–40.

Piromallo, C., D. Gasperini, P. Macera, and C. Faccenna (2008), A late Cretaceous contamination episode of the European-Mediterranean mantle, *Earth Planet. Sci. Lett.*, *268*, 15–27, doi:10.1016/j.epsl.2007.12.019.

Pischiutta, M., M. Anselmi, P. Cianfarra, A. Rovelli, and F. Salvini (2013), Directional site effects in a non-volcanic gas emission area (Mefite d'Ansanto, southern Italy): Evidence of a local transfer fault transversal to large NW-SE extensional faults?, *Phys. Chem. Earth*, *63*, 116–123, doi:10.1016/j.pce.2013.03.0082013.

Reyners, M., D. Eberhart-Phillips, and G. Stuart (1999), A three dimensional image of shallow subduction: Crustal structure of the Raukumara Peninsula, New Zealand, *Geophys. J. Int.*, *137*, 873–890.

Roure, F., P. Casero, and R. Vially (1991), Growth processes and melange formation in the southern Apennines accretionary wedge, *Earth Planet. Sci. Lett.*, *102*, 395–412, doi:10.1016/0012-821X(91)90031-C.

Sandrin, A., and H. Thybo (2008), Seismic constraints on a large mafic intrusion with implications for the subsidence history of the Danish Basin, *J. Geophys. Res.*, *113*, B09402, doi:10.1029/2007JB005067.

Scrocca, D., E. Carminati, and C. Doglioni (2005), Deep structure of the southern Apennines, Italy: Thin-skinned or thick-skinned?, *Tectonics*, *24*, TC3005, doi:10.1029/2004TC001634.

Scrocca, D., S. Sciamanna, E. Di Luzio, M. Tozzi, C. Nicolai, and R. Gambini (2007), Structural setting along the CROP-04-deep seismic profile (southern Apennines, Italy), in *Results of the CROP Project, Sub-Project CROP-04 Southern Apennines (Italy)*, Ital. J. Geosci., vol. 7, edited by A. Mazzotti, E. Patacca, and P. Scandone, Ital. J. Geosci., 283–296, Bollettino della Societa Geologica Italiana, Rome.

Seccia, D., C. Chiarabba, P. De Gori, I. Bianchi, and D. P. Hill (2011), Evidence for the contemporary magmatic system beneath Long Valley Caldera from local earthquake tomography and receiver function analysis, *J. Geophys. Res.*, *116*, B12314, doi:10.1029/2011JB008471.

Sella, M., T. Turci, and A. Riva (1988), Sintesi geopetrolifera della Fossa Bradanica (Avanfossa della catena appenninica meridionale), *Mem. Soc. Geol. Ital.*, *41*, 87–107.

Shiner, P., A. Beccaccini, and S. Mazzoli (2004), Thin-skinned versus thick-skinned structural models for Apulian carbonate reservoirs: Constrains from the Val d'Agri Fields, southern Apennines, Italy, *Mar. Pet. Geol.*, *21*, 805–827, doi:10.1016/j.marpetgeo.2003.11.020.

Spada, M., I. Bianchi, E. Kissling, N. Piana Agostinetti, and S. Wiemer (2013), Combining controlled-source seismology and receiver function information to derive 3-D Moho topography for Italy, *Geophys. J. Int.*, *194*(2), 1050–1068, doi:10.1093/gji/ggt148.

Speranza, F., and M. Chiappini (2002), Thick-skinned tectonics in the external Apennines, Italy: New evidence from magnetic anomaly analysis, *J. Geophys. Res.*, *107*(B11), 2290, doi:10.1029/2000JB000027.

Steckler, M. S., N. Piana Agostinetti, C. K. Wilson, P. Roselli, L. Seeber, A. Amato, and A. Lerner-Lam (2008), Crustal structure in the southern Apennines from teleseismic receiver functions, *Geology*, *36*(2), 155–158, doi:10.1130/G24065A.1.

Thurber, C. H. (1983), Earthquake locations and three-dimensional crustal structure in the Coyote Lake area, central California, *J. Geophys. Res.*, *88*, 8226–8236, doi:10.1029/JB088iB10p08226.

Thybo, H., and C. A. Nielsen (2012), Seismic velocity structure of crustal intrusions in the Danish Basin, *Tectonophysics*, *572*(573), 64–65, doi:10.1016/j.tecto.2011.11.019.

Toomey, D. R., and G. R. Foulger (1989), Tomographic inversion of local earthquake data from the Hengill Grensdalur central volcano complex, Iceland, *J. Geophys. Res.*, *94*, 17,497–17,510, doi:10.1029/JB094iB12p17497.

Trippetta, F., C. Collettini, M. R. Barchi, A. Lupattelli, and F. Mirabella (2013), A multidisciplinary study of a natural example of a CO_2 geological reservoir in central Italy, *Int. J. Greenhouse Gas Control*, *12*, 72–83, doi:10.1016/j.ijggc.2012.11.010.

Valoroso, L., L. Improta, P. De Gori, and C. Chiarabba (2011), Upper crustal structure, seismicity and pore pressure variations in an extensional seismic belt through 3D and 4D *Vp* and *Vp/Vs* models: The example of the Val d'Agri area (southern Italy), *J. Geophys. Res.*, *116*, B07303, doi:10.1029/2010JB007661.

Valoroso, L., L. Chiaraluce, D. Piccinini, R. Di Stefano, D. Schaff, and F. Waldhauser (2013), Radiography of a normal fault system by 64,000 high-precision earthquake locations: The 2009 L'Aquila (central Italy) case study, *J. Geophys. Res. Solid Earth*, *118*, 1156–1176, doi:10.1002/jgrb.50130.

Virieux, J., and V. Farra (1991), Ray tracing in 3D complex isotropic media: An analysis of the problem, *Geophysics*, *56*, 579–594.

Vitale, S., F. Dati, S. Mazzoli, S. Ciarcia, V. Guerriero, and A. Iannace (2012), Modes and timing of fracture network development in poly-deformed carbonate reservoir analogues, Mt. Chianello, southern Italy, *J. Struct. Geol.*, *37*, 223–235, doi:10.1016/j.jsg.2012.01.005.

Westaway, R., and J. Jackson (1987), The earthquake of 1980 November 23 in Campania-Basilicata (southern Italy), *Geophys. J. R. Astron. Soc.*, *98*, 375–443.